Revisiting the crustal structure and kinematics of the Central Andes at 33.5°S : implications for the mechanics of Andean mountain-building.

Magali Riesner[1], Robin Lacassin[1], Martine Simoes[1], Daniel Carrizo[2], Rolando Armijo[1]

[1] Institut de Physique du Globe de Paris, Sorbonne Paris Cité, Univ Paris Diderot, UMR 7154 CNRS, F-75005 Paris, France.
[2] Advanced Mining Technology Center, Facultad de Ciencias Físicas y Matemáticas, Universidad de Chile, Santiago, Chile.

Corresponding author: Magali Riesner (riesner@ipgp.fr)

Abstract

The Andean belt is the only present-day active case example of a subduction-type orogeny. However, an existing controversy opposes classical views of Andean growth as an east-verging retro-wedge, against a recently proposed bi-vergent model involving a primary west-vergent crustal-scale thrust synthetic to the subduction. We examine these diverging views by quantitatively re-evaluating the orogen structural geometry and kinematics at the latitude of 33.5°S. We first provide a 3D-geological map and build an updated section of the east-vergent Aconcagua fold-and-thrust belt (Aconcagua-FTB), which appears as a critical structural unit in this controversy. We combine these data with geological constraints on nearby structures to derive a complete and larger scale section of the Principal Cordillera within the forearc region. We restore our section and integrate published chronological constraints to build an evolutionary model showing the evolving shortening of this forearc part of the Andes. The proposed kinematics implies uplift of the Frontal Cordillera basement since ~20-25 Ma, supported by westward thrusting over a crustal ramp that transfers shortening further west across the Principal Cordillera. The Aconcagua-FTB is evidenced as a secondary east-verging roof thrust atop the large-scale basement antiform culmination of the Frontal Cordillera. We estimate a shortening of ~27-42 km across the Principal Cordillera, of which only ~30% is absorbed by the Aconcagua-FTB. Finally, we combine these findings with published geological data on the structure of the eastern back-arc Andean mountain front, and build a crustal-scale cross-section of the entire Andes at 33.5° S. We estimate a total orogenic shortening of ~31-55km, mainly absorbed by crustal west-vergent structures synthetic to the subduction. Our results provide quantitative key geological inferences to revisit this subduction-type orogeny and compare it to collisional alpine-type orogenic belts.

Key Points:

- 3D structural map and revisited geological cross-section of the Aconcagua fold-and-thrust belt at 33°S and 33.5°S.
- Kinematics of crustal deformation and shortening of the Central Andes at 33.5 °S since ~20-25 Ma.
- Bi-vergent crustal-scale model of the Andes at 33.5°S with a total orogenic shortening of ~31-55km.

1. Introduction

It is now generally admitted that orogeny on Earth results primarily from tectonic shortening and thickening of continental crust associated with continuing plate convergence, most commonly after a protracted period of subduction of oceanic lithosphere under continental lithosphere. Two end-members are generally distinguished: (1) the collision-type (or Himalayan-type) orogeny, like the European Alps or the Himalayas, and (2) the subduction-type (or Andean-type) orogeny, observed in the western Cordilleras of North-America or the Central Andes of South-America. Collision-type mountain belts form where the subducted oceanic plate carries behind another continent, leading eventually to lithospheric-scale collision of two continental plates. In some rare cases, collision follows the subduction of a domain of exhumed mantle after a period of intra-continental rifting, such as proposed for the European Pyrenees *(e.g. Mouthereau et al., 2014)*. In any of these cases of collisional orogens, a bivergent orogenic wedge subsequently develops along the plate boundary, where primary crustal thrusts form a detached pro-wedge synthetic to the continuing subduction process of the lithospheric mantle slab. This type of process is documented by abundant data and has been extensively conceptualized and modeled *(e.g. Davis et al. 1983, Malavieille 1984, Willett et al. 1993, Tapponnier et al. 2001, McClay and Whitehouse 2004, Graveleau et al. 2012)*. On the other hand, the subduction-type (or Andean-type) orogeny forms after an initial period of oceanic subduction involving crustal extension within the continental back-arc, associated with slab retreat and roll-back. This initial stage is followed by a protracted period of mountain building within the upper continental plate. The later process involves significant crustal shortening, probably related to the relatively young age of the subducting plate *(e.g., Molnar and Atwater, 1978; Capitanio et al., 2011)* and to stability or net advance of the trench towards the upper continental plate *(e.g., Schellart et al. 2007, Husson et al. 2012, Faccenna et al. 2013)*. For subduction-type orogens, however, mechanical models exploring driving processes and associated boundary conditions have not yet convincingly explained the partitioning of the continuing plate convergence between oceanic subduction and upper-plate orogenic processes. The former absorbs much of the convergence and is associated with significant seismicity at the inter-plate interface, and the latter absorbs a small fraction of the convergence across the continental margin but generates over the long term significant crustal shortening and topography.

The archetypical Central Andes is a well-described present-day active subduction-type orogen (Figure 1). In the case of this belt, however, contrasting tectonic models have been proposed over the last decades *(e.g. James 1971, Kono et al. 1989, Lyon-Caen et al. 1985, Isacks 1988)*, implying different reconstructions of crustal thickening processes and different interpretations of its structural evolution. The evolution of these models has led to the overall present-day idea that the Andean orogen has grown by diachronic eastward thrust propagation within an east-verging retro-wedge, toward the continent *(e.g. Suárez et al. 1983, Kley 1999, Ramos et al. 2004, Farías et al. 2010, Giambiagi et al. 2014)*. However, the possible contribution of a counterbalancing pro-wedge, synthetic to the Nazca - South America subduction zone, defining a bi-vergent structure for the Central Andes *(Armijo et al., 2010, 2015)* appears understated.

The aim of this work is to revisit a critical tectonic section at 33.5°S latitude near the southern end of the Central Andes. The Andes are characterized by obvious lateral latitudinal variations in width, structure and total shortening (Figure 1) *(Ramos et al. 2004, Giambiagi et al. 2012)*, either related to varying boundary conditions along the subduction zone and within the upper plate *(e.g. Russo and Silver 1994, Charrier et al. 2007, Schellart et al., 2007, Capitanio et al., 2011)*, or to variable rates and timing of deformation *(e.g. Oncken et al. 2006, 2013 Faccenna et al. 2017, Armijo et al. 2015)*. Total shortening estimates vary laterally, and increase from <100 km at ~33.5 °S *(Ramos et al. 2004; Giambiagi et al. 2012; Armijo et al. 2010; Giambiagi et al. 2014)* to ≥ 400 km at ~20°S *(McQuarrie et al. 2005; Lamb 2011; Armijo et al. 2015)*, with the northward progressive implication of several structural units (namely the Precordillera, Eastern Cordillera and Sub-Andean belt) to crustal shortening. By 33.5° S, the Andean belt is narrower and structurally much simpler than further north (Figure 1), since it is constituted only of the Principal and Frontal Cordilleras. This makes this section a good target to study first-order Andean mountain-building processes. Furthermore, at this latitude, conflicting interpretations of geological observations have originated the ongoing debate on east-vergent versus bi-vergent orogeny. The east-vergent model remains widely accepted *(e.g., Ramos et al. 2004,*

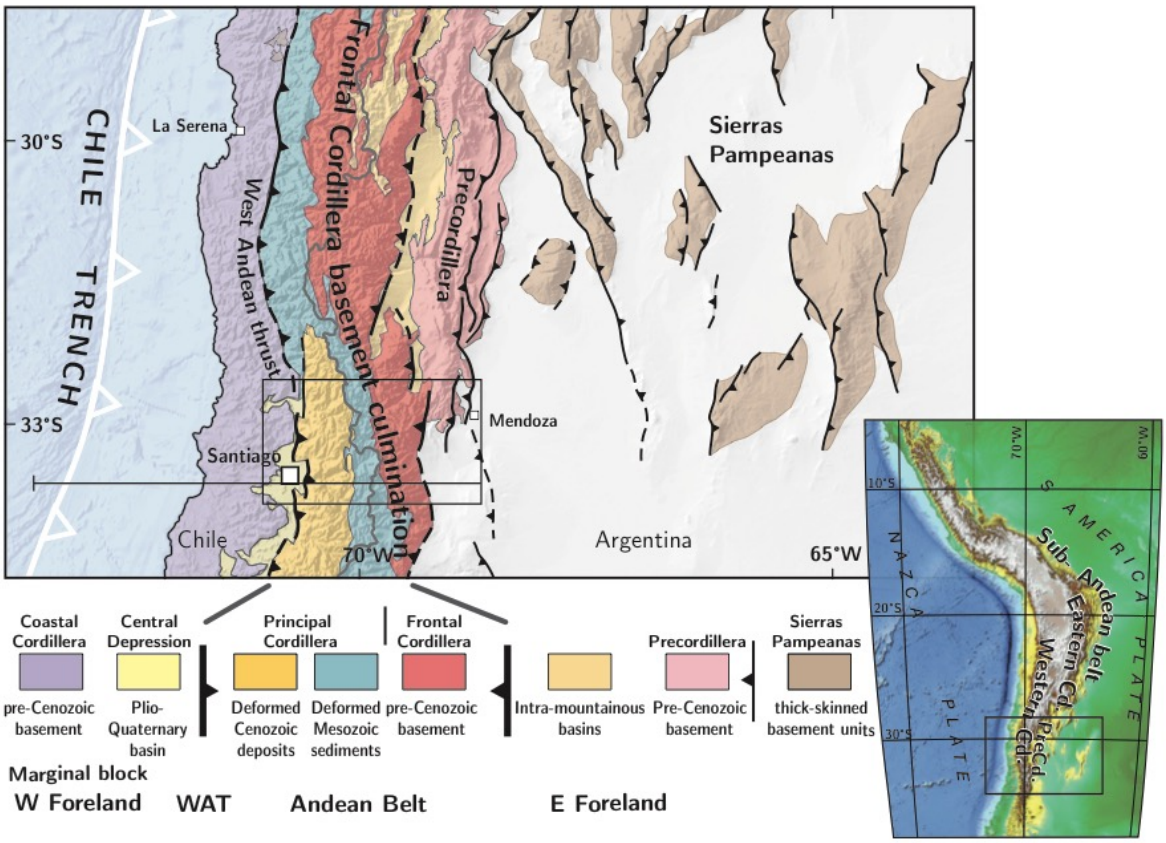

Figure 1: Physiography and first-order geology of the subduction margin of the Andes in central Chile and westernmost central Argentina. To the west, the trench marks the Nazca-South America plate boundary, reported in white with open triangles. East of the trench, the subduction margin is composed, from west to east, of the Coastal Cordillera, the Central Depression, and the Andean belt. The mountain belt, ~145km wide at 33.5°S, is composed of the folded Mesozoic (green) and Cenozoic (yellow) sedimentary and volcanic rocks forming the Principal Cordillera, and to the east, of the Andean basement backbone culmination forming the Frontal Cordillera (red). North of 33°S, the Andean mountain belt becomes significantly wider eastward with the addition of the basement thrust sheets of the Pre-Cordillera (pink) and of the Sierras Pampeanas (brown). Black rectangle locates our study area (Figure 3), and the black line our final cross-section (Figure 10).

Giambiagi et al. 2003, 2014, Farías et al. 2010) (Figure 2a). It is chiefly based on the description of the Andean eastern front and on the Aconcagua fold-and-thrust belt (hereafter Aconcagua-FTB), a renowned east-vergent structure in the high cordillera, juxtaposed between the volcanic arc and the basement culmination formed by the Frontal Cordillera *(e.g., Ramos 1988, Ramos et al., 1996a, 2004, Cegarra and Ramos, 1996, Giambiagi and Ramos 2002, Giambiagi et al. 2003)*. According to widely admitted east-vergent interpretations for the formation of the Andes, the Aconcagua-FTB represents an early deformation front of the Andes, consistent with an eastward propagating system (Figure 2a). More precisely, the east-vergent model implies two major stages (see evolutionary model from *Giambiagi et al., 2014*): (1) an early stage of uplift and deformation of the Aconcagua-FTB from ~25 to ~10 Ma; and (2) a late stage from ~10-9 Ma to the present-day, with the Andean frontal deformation propagating eastward and initiating the late uplift of the Frontal Cordillera basement culmination along the eastern front of the Andes (Figure 2a). On the other hand, the recent discovery of the active west-vergent San Ramón Fault (33.5°S) and of large west-vergent thrusts along the Western Andean front *(Armijo et al., 2010; Vargas et al., 2014; Riesner et al., 2017)*, has prompted the emergence of an alternative model suggesting that Andean crustal thickening at this latitude has been supported mainly by west-vergent thrusts *(Armijo et al 2010)*. These structures are proposed to root into a major east-dipping west-vergent thrust ramp (the West Andean Thrust or WAT) under the basement high of the Frontal Cordillera, which is interpreted as forming a large-scale basement antiform culmination on top of this crustal ramp (Figure 2b). In this bi-vergent view, the Aconcagua-FTB is interpreted as a secondary back-thrust feature of a much larger west-vergent West Andean Fold-and-Thrust Belt (hereafter West Andean-FTB;

Armijo et al. 2010; Riesner et al. 2017). The bi-vergent model implies continuous and primarily westward-propagating shortening across the Andes, and early uplift of the main Andean basement culmination of the Frontal Cordillera, initiating ~20-25 Myr ago (Figure 2b).

To discriminate between the two foregoing models, we focus on reassessing the structural and chronological evolution of the Central Andes in the region where both the Aconcagua-FTB and the West Andean-FTB are present (Figures 1 and 2). Our approach will subsequently follow a reasoning where structural and geological field observations at 33.5°S are first re-evaluated at the scale of individual tectonic units, before integrating and up-scaling our interpretations to a larger regional and finally crustal scale section across the Andes at this latitude. More precisely, as a first step, we hereafter quantify precisely the structural geometry and kinematics characterizing the emblematic Aconcagua-FTB observable between 32.5°S and 34°S (Figure 3), and the region east and west of it. These data allow for building two structural cross-sections of the Aconcagua-FTB at ~33°S and ~33.5°S, which are subsequently discussed in light of previously published sections. Then, at a regional scale, we integrate and evaluate the contribution of the Aconcagua-FTB, relative to other structural units of the Andean forearc, to describe the geometry of the western flank of the Andes (Principal Cordillera). Using published chronological constraints, our section is incrementally restored and tested. Finally, we upscale our reasoning, and integrate geological, geophysical and chronological constraints at the scale of the whole orogen at 33.5°S. In particular, we discuss the timing of the initiation of the tectonic uplift of the Frontal Cordillera basement culmination using recently published thermochronological data *(Hoke et al., 2014)* and additional constraints on the Andean eastern front *(Garcia et al. 2005, Garcia and Casa 2014 and Giambiagi et al. 2015)* to discriminate between the two existing conceptual models of Andean orogeny. These constraints allow us for discussing the mechanics of Andean mountain-building and for proposing a crustal-scale section of the Andes at this latitude.

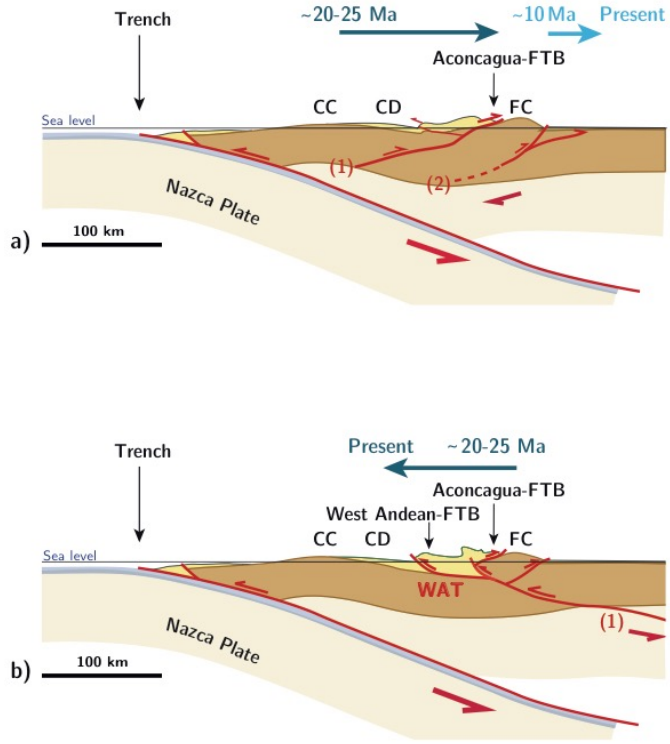

Figure 2: Two conflicting conceptual models of the Andes at ~33.5°S latitude.
a) East-vergent model proposed by Giambiagi et al. (2014) in which the Aconcagua FTB is a major former frontal structure, overthrusting the Frontal Cordillera basement high. This model implies a first tectonic phase from ~25 to ~10Ma (dark blue) with deformation and uplift of the forearc basin and of the Aconcagua FTB, and coeval subsidence of the eastern foreland basin where the current Frontal Cordillera is located. Then, during the second phase, from ~10 Ma to present (light blue), the deformation propagates eastwards, with a late exhumation of the Frontal Cordillera.
b) Bi-vergent orogen model with a dominant westward primary vergence proposed by Armijo et al. (2010). In this model, the Aconcagua FTB is a secondary structure, passively transported over the Frontal Cordillera basement high. This model implies a continuous westward deformation of the mountain belt over the last ~20-25 Myr. In this case, the exhumation of the Frontal Cordillera basement high initiated early and has been continuous since ~20-25 Ma.
CC: Coastal Cordillera; CD: Central Depression; West Andean-FTB: West Andean fold-and-thrust belt; FC: Frontal Cordillera; Aconcagua-FTB: Aconcagua fold-and-thrust belt; WAT: West Andean Thrust.

2.Geological setting

*2.1.*General description.

The Central Andes extend over 4000 km from northern Peru to central-southern Chile, and result from the subduction of the Nazca Plate under the South American Plate. Our study area is located between ~33°S and ~33.5°S, at the latitude of Santiago de Chile (Chile) and Mendoza (Argentina) (Figure 1). There, the

Andes mountain belt is ~100 to 160 km km wide and reaches average altitudes of ~5000m (up to 6962m at the Aconcagua). Towards the west, it is facing a western foreland made of: (1) the Chilean Central Depression (CD) at ~500m above sea level and filled by less than 1km of Quaternary sediments; (2) the Coastal Cordillera (CC) constituted of Paleozoic and Mesozoic rocks with altitudes commonly below 2000m, and (3) the offshore continental margin just in front of the Chile trench (Figure 1). To the far east of the Andes, the southern Sierras Pampeanas (Figure 1) are thick-skinned west-vergent structures outcropping pre-Andean basement rocks, with relatively limited amount of cumulative shortening at ~33°S latitude and further south. They are further described by *Ramos et al. (2002)* and will not be further considered here.

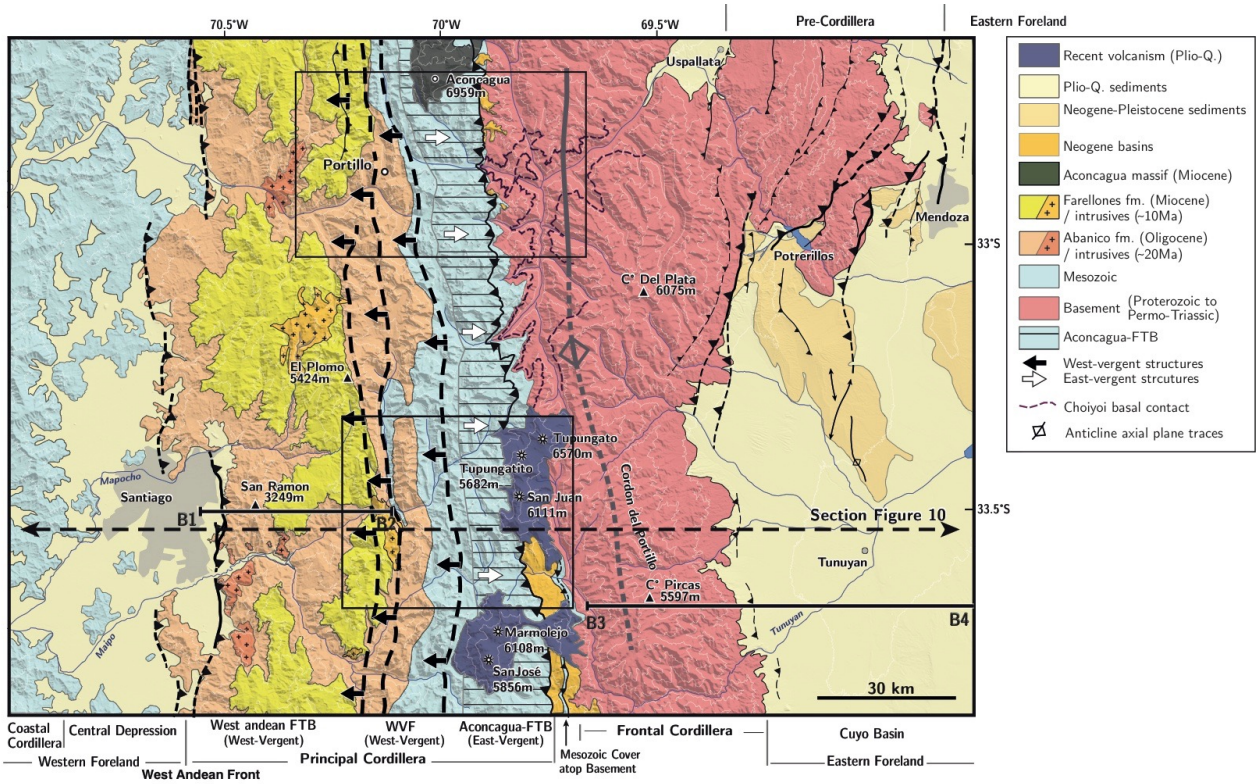

Figure 3: Structural map of the Andes over our study region (location on Figure 1) compiled from geological maps of the Chilean and Argentinian Andes *(Polanski, 1964, 1972 ; Thiele, 1980 ; Gana et al., 1999 ; Fock, 2005, Rivano et al, 1993, SEGEMAR, 2000, 2010, SERNAGEOMIN, 2003, Giambiagi 2001 ; Giambiagi and Ramos 2001, Armijo et al., 2010, Riesner et al., 2017)* and from our own field observations. Rectangles locate our detailed mapping areas to the north (Figure 4) and to the south (Figure 5) of the Aconcagua fold-and-thrust belt. Sections B1-B2 (Riesner et al 2017) and B3-B4 (portion of the section from Giambiagi et al., 2014, used for our general section of Figure 10) are also reported. Sections within the detailed mapping areas are located in Figures 4 and 5. The thick dashed line locates part of the section of Figure 10 (see complete location Figure 1). FTB : fold-and-thrust belt ; WVF : West-Vergent Folds.

In our study region (Figure 3), the Andes themselves are composed of three principal structural units: (1) to the west, the Principal cordillera (PC) is constituted of a deformed ~12-15 km thick sequence of early Jurassic to Miocene sedimentary rocks, topped by Oligo-Miocene volcanic and volcano-clastic rocks *(e.g., Thiele 1980, Mpodozis and Ramos, 1989, Charrier et al. 2007, Armijo, 2010)*; (2) further east, the basement culmination of the Argentinian Frontal Cordillera (FC) is composed of pre-Andean units of Early-Mid Paleozoic to Permo-Triassic age *(e.g., Mpodozis and Ramos, 1989, Gregori et al.,1996, Giambiagi et al. 2003, Heredia et al. 2012)*; and (3) to the north-east (only north of ~33°S), the Pre-Cordillera forms the eastern front of the Andes and is constituted of Early-Mid Paleozoic to Permo-Triassic basement rocks *(Giambiagi et al. 2011; Allmendinger and Judge 2014; Fosdick et al. 2015)*. Because our final cross-section synthesizes observations at 33.5°S, the Pre-Cordillera will not be considered hereafter.

2.2. Geology of the Principal Cordillera

The Principal Cordillera includes the west-vergent West Andean-FTB to the west *(Riesner et al 2017)* and the east-vergent Aconcagua-FTB on its eastern side *(Ramos et al., 1996a, 2004, Giambiagi et al., 2001,Giambiagi 2003)*. These two belts are separated by vertical folded series, interpreted as tight west-vergent folds (hereafter WVF) by Armijo et al. (2010) (Figure 3). The Principal Cordillera is composed of the Oligocene and Miocene Abanico and Farellones formations within the West Andean-FTB *(Charrier 2002, 2005)* and of Mesozoic series within the WVF and Aconcagua-FTB (Figure 3). The Abanico formation bears volcaniclastic rocks, tuffs, basic lavas, ignimbrites and interbedded alluvial, fluvial and lacustrine sediments *(Charrier 2002, 2005)*. At the latitude of this study, K/Ar and $^{40}Ar/^{39}Ar$ ages on plagioclase, in ash flows and lavas from this formation range from 30.9 to 20.3 Ma. It is intruded by porphyric dykes as young as 16.7 Ma (*Gana et al., 1999; Aguirre et al. 2000, Nyström et al., 2003; Vergara et al., 2004)*. The Farellones formation is ~1-2 km thick, composed of intermediate and basic lava flows with volcanic rocks and minor ignimbrite flows *(Beccar et al., 1986; Vergara et al., 1988*). K/Ar, $^{40}Ar/^{39}Ar$ ages on biotite and plagioclase and U/Pb ages on zircon range from ~21.6 to ~16.6 Ma in ash flows and lavas of this formation (*Beccar et al., 1986; Nyström et al., 2003; Deckart et al., 2005*). The contact between these two formations is described as progressive and unclear as they are both composed of volcanic and volcano-clastic sediments (*Charrier et al., 2002, 2005*). However, at a regional scale, the limit between the two units is illuminated by an angular unconformity *(Armijo et al., 2010; Riesner et al, 2017)*.

2.2.1.The West-Andean fold-and-thrust belt

Recently, Riesner et al. (2017) proposed a detailed 3D map and cross-section of the West Andean-FTB (section B1-B2 on Figure 3), and quantified the kinematics of this fold-and-thrust belt by combining structural observations and chronological constraints. The Abanico and Farellones formations are folded by a succession of four to five west-vergent faults that root onto a ~12-15 km deep décollement at the base of the Meso-Cenozoic series and that absorbed a total shortening of 9-15 km. The derived kinematics suggests that the West Andean-FTB evolved following a classical forward (here westward) propagating system of faults and folds over the last ~20-25 Myr, with a long-term shortening rate of 0.1-0.5 mm/yr. The San Ramón Fault, at the western front of the West Andean-FTB nearby Santiago de Chile, appears presently seismically active *(Armijo et al. 2010, Vargas et al. 2014)*.

2.2.2.The West-Vergent Folds

To the east of the West Andean-FTB, two interpretations have been proposed for the deformation of the thick Jurassic to Miocene series. Following several authors these series are interpreted as being duplicated by numerous east-vergent thrusts, forming large thrust sheets structurally associated with the Aconcagua-FTB *(e.g., Cegarra and Ramos 1996, Giambiagi and Ramos 2002, Farías et al. 2010)*. In an alternative structural model, the Abanico and Farellones formations are described as folded within a series of large and asymmetric west-verging folds *(Thiele 1980, Rivano et al., 1993; Armijo et al., 2010)*. These folds expose further east the complete Mesozoic sedimentary sequence within a ~5-7 km wide nearly vertical fold limb (Figure 3) *(Thiele, 1980; Armijo et al., 2010)*, with an overall large-scale top-to-the-west stratigraphic geometry. As explained further in this paper (section 3.3), the second interpretation will be subsequently favored after integrating these structures at a larger scale, i.e. at the scale of the entire Principal Cordillera. We will therefore subsequently use the terminology of West-Vergent Folds (WVF) to refer to this specific structural unit. From west to east, this Mesozoic series is constituted of the conglomeratic and volcano-clastic Cretaceous Colimapu formation, the Late Jurassic-Early Cretaceous calcareous Lo Valdés formation, and the ~3 km thick continental conglomerates, andesitic lavas and breccias of the Late Jurassic Río Damas Formation. At the base of the Meso-Cenozoic series a regionally well-known gypsum layer is located in the Río Colina formation ("Yeso Principal", *Thiele 1980*). These formations show evidence of green schist burial metamorphism *(Robinson et al., 2004)*. Overall, in the western side of the Andean Basin, the Meso-Cenozoic series are ~9-10 km thick.

2.2.3.The Aconcagua fold-and-thrust belt

Further east, the Mesozoic series thins within the Aconcagua-FTB (Figure 3) where several studies have described sedimentary series with facies different from those observed further west within the WVF *(Thiele, 1980; Giambiagi, 2000; Giambiagi et al., 2003)*. Based on stratigraphic studies, *Groeber (1918)* suggested the existence of a paleogeographic high for the Aconcagua area, known as the Alto del Tigre. The Mesozoic sediments composing the Aconcagua-FTB (in particular the Mendoza Group – *Giambiagi et al., 2003*) are indeed characteristic of shallow platform environments *(Aguirre-Urreta, 1996, Aguirre Urreta and Alvarez, 1998 cited in Giambiagi et al. 2003b)*. Such structural high, called the Aconcagua Platform by *Mpodozis and Ramos (1989)*, existed during deposition of the Late Jurassic-Early Cretaceous Mendoza Group as demonstrated by the stratigraphic analysis of *Lo Forte (1992)* cited in *Ramos et al. (1996a)*. Late Jurassic gypsum layers are abundant and form diapirs within the Aconcagua-FTB (e.g. in the Valle del Yeso, *Thiele, 1980*; note that "Yeso" means "gypsum" in Spanish).

The Aconcagua-FTB corresponds to a ~20km wide zone of east-vergent thrusts that overthrust syntectonic Neogene intra-mountainous basins and the large basement high of the Frontal Cordillera *(Ramos 1988, Ramos et al. 1996a, Giambiagi et al., 2001, 2003, Giambiagi and Ramos, 2002)* (Figure 3). Interpretations of the Aconcagua-FTB vary, in particular in terms of cumulative shortening, depth of the basal décollement and structural contribution of this fold-and-thrust belt to Andean mountain building. Immediately south of the Aconcagua (Argentina), the Aconcagua-FTB is described as a thin-skinned thrust belt separated from the basement by a shallow basal detachment located in a Jurassic gypsum layer at ~2-3 km depth *(Ramos, 1988, Cegarra and Ramos, 1996)*. The estimates of cumulative shortening vary widely from ~20-25 km (measured on section of Figure 12 in Ramos, 1998) to 62.7 km *(Cegarra and Ramos, 1996)*. About 80 km further south, on a section along the Yeso (Chile) and Palomares (Argentina) valleys, *Giambiagi and Ramos (2002) and Giambiagi et al. (2003)* suggested that the Aconcagua-FTB roots deeper (5 to 10 km) into the Paleozoic basement. These authors estimate the cumulative shortening to be 47 km *(Giambiagi and Ramos, 2002)*. Alternatively, *Armijo et al. (2010)* propose that shortening on the Aconcagua-FTB would be at most 10 km. We also already noted that the steep top-to-the-west, Miocene to Mesozoic series forming the WVF of *Armijo et al. (2010)*, had also been interpreted as thrust-sheets belonging to the Aconcagua-FTB *(Cegarra and Ramos, 1996, Giambiagi and Ramos, 2002)*, leading to drastic differences in shortening estimates. We will discuss this issue in more detail afterward.

Despite differences in the details of interpreted structures, all east-vergent models view the Aconcagua-FTB as a former Andean deformation front, active from ~21 to ~10 Ma, as retrieved from the ages of the synorogenic conglomerates of overthrusted intra-mountainous basins, before deformation propagated east of the Frontal Cordillera *(Giambiagi et al., 2003; Ramos et al., 2004; Giambiagi et al., 2014)*. Given this, the Aconcagua-FTB and Frontal Cordillera eastern frontal thrust are interpreted as two successive major frontal thrusts during Andean orogeny (Figure 2a). Alternatively, *Armijo et al. (2010)* considered the Aconcagua-FTB as a minor feature of the Andes, passively transported over the basement high of the Frontal Cordillera, as this latter has been continuously uplifted over a deep west-vergent ramp for the last ~20-25 Myr (Figure 2b).

2.3. The Frontal Cordillera and Cuyo Basin

To the east, the Frontal Cordillera basement high is composed of Choiyoi Group rocks (Permian-Triassic) unconformable over the Paleozoic Gondwanan basement, with a core of Proterozoic metamorphic rocks (Figure 3) *(Polanski, 1964, 1972; Giambiagi et al., 2003; Gregori et al., 1996, Heredia et al., 2012; SEGEMAR, 2010)*. Protero-Paleozoic units are affected by a series of complex basement faults that are known to have been at some places reactivated during Andean orogeny, in particular to the north of our study area, along the eastern front of the Andes and within the Pre-Cordillera *(Giambiagi et al., 2011)*. These basement faults are however essentially sealed by the unconformable Permo-Triassic Choiyoi series, in particular along our section at 33.5°S. As such, this unconformable contact, mapped in Figure 3, can be used to mark and delineate the Andean deformation of the Frontal Cordillera basement. *Armijo et al. (2010)* propose that this contact outlines a broad ~30-50 km wide antiformal culmination, associated to Andean deformation and

mountain-building.

At this latitude, the Cuyo basin to the east of the Frontal Cordillera represents the eastern foreland of the Andes (Figures 3). This basin is relatively shallow and composed of more than 3 km thick Cenozoic sediments dated from ~16 Ma *(Yrigoyen, 1993; Irigoyen et al., 2000; Garcia and Casa, 2014)*, deposited over the Permian-Triassic basement of the San Rafael block *(Llambias et al., 2003; Mpodozis and Ramos 1989)*. Reactivation of Permo-Triassic extensional structures within the basement lead to Andean inversion of the Cuyo basin *(Ramos et al 1996b, Charrier et al., 2007)*. Such inversion is proposed to have initiated by ~4-7 Ma, as derived from geological constraints based on the seismic lines of *Garcia et al. (2005), Garcia and Casa (2014) and Giambiagi et al. (2015)*, and is currently active. The shortening across the Cuyo basin is estimated to be quite minor south of the Pre-Cordillera termination *(Ramos et al., 1996a)*, between ~2 and ~4 km *(Garcia et al., 2005; Garcia and Casa, 2014; Giambiagi et al., 2015)*.

As mentioned previously, the two existing conceptual models proposed for the Andes tectonic evolution at this latitude imply different timing for the uplift of the Frontal Cordillera basement high (Figure 2). Indeed, the east-vergent model implies that deformation propagated from the Aconcagua-FTB to the Frontal Cordillera thrust after ~10-9 Ma, thus initiating uplift and exhumation of the Frontal Cordillera by this time *(e.g. Giambiagi et al., 2014)* (Figure 2a). On the other hand, the bi-vergent model of Armijo et al. (2010) implies continuous and westward-propagating shortening across the Andes, with an early initiation of uplift of the Frontal Cordillera by ~20-25 Ma, supported by a west-vergent crustal ramp (Figure 2b). The exhumation of the Frontal Cordillera has been investigated in provenance studies of the intra-mountainous basins located between the Principal and Frontal Cordilleras (Figure 3) and from thermochronological ages. In particular, the presence of clasts originated from both the Principal and the Frontal Cordilleras in the sedimentary clastic sequences of the Alto Tunuyan intra-mountainous basin has been noted for a long time, since Darwin *(see for example p.182 in Darwin, 1846)*. Recently, zircons with affinities to the Paleo-Proterozoic basement and Permo-Triassic Choiyoi units of the Frontal Cordillera, early in the clastic series of this basin, have been interpreted to "correspond to recycled material within the Mesozoic units [of the Principal Cordillera] or else to a direct supply from a paleorelief at the current position of the Frontal Cordillera" *(Porras et al., 2016)*. Recent thermochronological constraints on the exhumation of the Frontal Cordillera tend to support the second interpretation as they suggest that the uplift and exhumation of the Frontal Cordillera initiated early by ~25 Ma, and that it accelerated recently by ~10 Ma *(Hoke et al 2014)*. This early initiation of uplift has recently been corroborated by a new thermochronological dataset *(Riesner 2017)*. Such an early uplift, since ~25 Ma, implies that the intra-mountainous basins between the Aconcagua-FTB and the Frontal Cordillera were never part of a continuous basin connected to the eastern Cuyo foreland basin, but rather deposited in isolated sub-basins between already uplifted topographic highs *(Hoke et al., 2014)*.

3. Re-assessing the structural geometry of the Aconcagua fold and thrust belt

To further constrain Andean mountain-building (Figure 2), we propose to first re-assess the structural geometry and cumulative shortening of the Aconcagua-FTB, with a particular emphasis on its structural continuity with other structural elements west (West Andean-FTB and WVF) and east (Frontal Cordillera) of it. This will allow for an accurate re-assessment of the structural position of this fold-and-thrust belt within the Andes, and consequently, for a re-appraisal of the kinematics of Andean mountain-building at the latitude of our cross-section (Figure 2).

3.1 Building a structural map of the West-Vergent Folds, Aconcagua fold-and-thrust belt and western Frontal Cordillera.

We first define two main areas that appear most appropriate to investigate the structure and kinematics of the Aconcagua-FTB (Figure 3). The area south of the Aconcagua volcano (Argentina) (Figure 4) is particularly suitable for our study as geometries are well exposed, and this is where the Aconcagua-FTB has been described (e.g., Ramos 1988). Geological sections of the Aconcagua-FTB in this area have been published, allowing for comparing our results with those previously obtained *(Ramos et al., 1988; Cegarra*

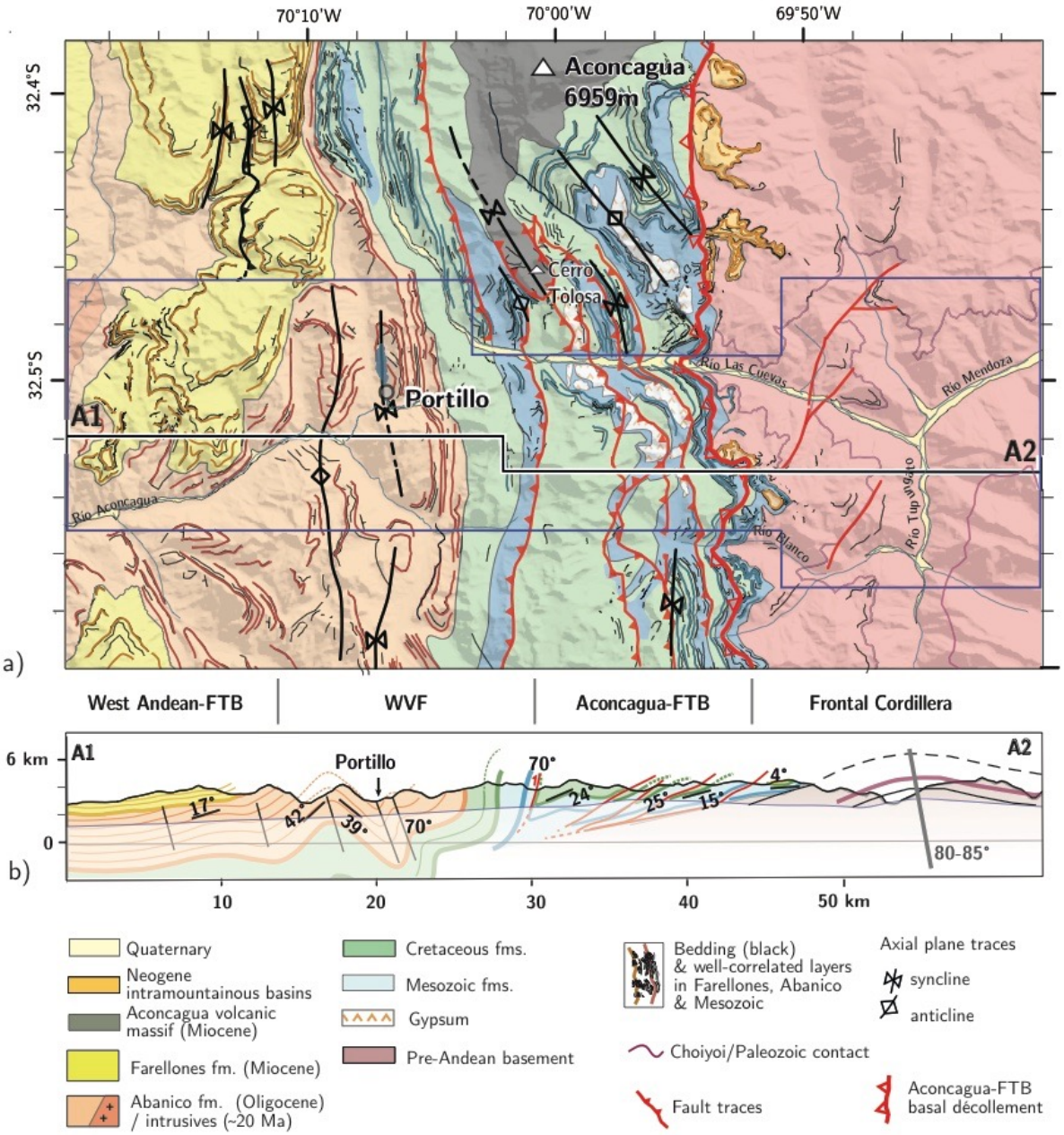

Figure 4 : (a) Structural map of the Aconcagua fold-and-thrust belt (AFTB) at ~33°S (see location on Figure 3), derived from a compilation of published geological maps *(Rivano et al, 1993, SEGEMAR, 2000, SERNAGEOMIN, 2003, Ramos 1996b, Ramos 1988)* and field observations. Structural and geological data are overlaid on Aster DEM. Bedding traces (thin grey lines) are mapped from satellite images and aerial photographs. Thicker lines mark bedding traces that correlate well over several kilometers in Abanico (red lines), Farellones (yellow lines) formations and in Mezosoic series (blue lines). Major anticlinal and synclinal axes are represented by black arrowed lines, and major outcropping faults are represented by red lines with triangles. Areas marked by dark blue rectangles correspond to the swaths used for projecting bedding traces on section A1-A2 (see further details on our approach in main text). Note that we interpret the Cerro Tolosa as a volcanic deposit related to the Aconcagua volcano. WVF: West-Vergent Folds; FTB: Fold-and-Thrust Belt**. (b)** Synthetic sub-surface cross-section deduced by projecting bedding geometries along section A1-A2 (Figure 4a). Direct surface observations are possible from mountain tops down to valley bottoms. Blue line reports río Aconcagua, Las Cuevas and Mendoza river profiles that define the limit between directly observed structures (clear colors above) and extrapolations at depth (transparency below).

and Ramos, 1996; Ramos et al., 1996b). We also map structures within the Yeso and Palomares valleys, at the latitude of Santiago (Chile) and Tunuyan (Argentina) (Figure 5). Bedding attitudes are less clear in this region due to the presence of gypsum diapirs that disrupt structural geometries. However, our results can be

compared to previously published sections *(Thiele et al., 1980; Giambiagi and Ramos 2002, Giambiagi et al., 2001, 2003)*, and allow for testing for lateral structural continuity over all our study region (Figure 3).

We build detailed structural maps of the Aconcagua-FTB in both areas of our study region (Figures 4 and 5), following the methodological approach of *Riesner et al. (2017)*. We deliberately discard to rely on standard approaches using statistical analyses of numerous outcrop-scale (≤10 m) strike-and-dip measurements. Indeed, a large-scale observational approach, using carefully selected satellite images combined with digital topography, enables to identify the landscape-scale geometry and filters the noise associated with volcanic, volcano-clastic depositional environments, or local secondary structural

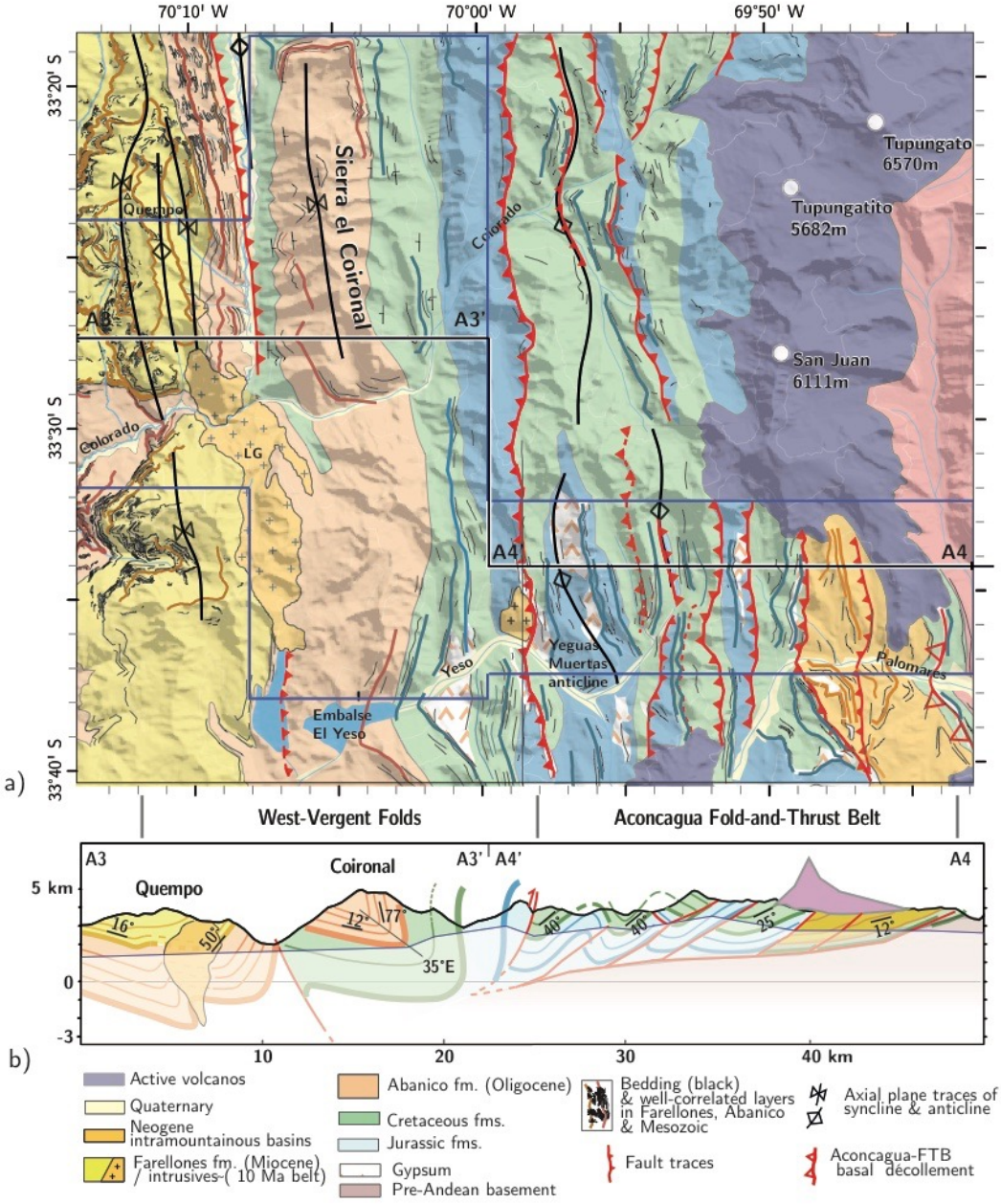

Figure 5: (a) Structural map of the Aconcagua fold-and-thrust belt at ~33.5°S derived from a compilation of published geological maps *(Polanski, 1964, 1972 ; Thiele, 1980 ; Fock, 2005, SEGEMAR, 2010, SERNAGEOMIN, 2003, Giambiagi 2001 ; Giambiagi and Ramos 2001; Giambiagi 2000; Armijo et al., 2010, Riesner et al., 2017)* and field observations (see location on Figure 3). See legend of figure 4 for additional details. **b)** Synthetic sub-surface cross-section deduced by projecting bedding geometries along the combined sections A3-A3' and A4'-A4 (Figure 5a). Direct surface observations are possible from mountain tops down to valley bottoms. Blue line reports Colorado and Palomares river profiles that define the limit between directly observed structures (clear colors above) and extrapolations at depth (transparency below). LG : La Gloria Pluton.

complexities associated for instance to gypsum diapirism (see *Riesner et al., 2017*, for further explanation of the methodology). This approach enables us to carefully map stratigraphic layers in 3D using high-resolution satellite images from the Google Earth database (Landsat 7, DigitalGlobe), aerial photographs and digital elevation models (Aster DEM, with ~30 m resolution). The satellite mapping is systematically checked in the field and combined with information from published geological maps *(Polanski, 1964, 1972; Thiele, 1980; Ramos 1988; Rivano et al., 1993; Ramos et al., 1996b; Giambiagi and Ramos 2002; Giambiagi, 2003; Giambiagi et al., 2001, 2003; Fock, 2005; SEGEMAR, 2000, 2010, Armijo et al., 2010)*. Altogether, these data allow for proposing a precise 3D geological and structural map of the two main areas of investigation (Figures 4 and 5), which displays in detail the geometry of the folded structure of the Aconcagua-FTB, as well as that of the WVF and of the Frontal Cordillera. Our geo-referenced 3D stratigraphic horizons are provided as supplementary materials for both the north and south areas (Data Set S1 and S2).

We pay a particular attention to the mapping of the contact between the Abanico and Farellones formations that in places appears as an angular unconformity. The transition between the nearly vertical Mesozoic series of the WVF and of the Aconcagua-FTB is mapped in detail. The deformation of the Frontal Cordillera basement high is emphasized within our northern area by the geometry of the regional unconformable contact between the pre-Andean Permo-Triassic Choiyoi series and the Paleozoic basement units (Figure 4). We recall here that we do not focus on the details of the Paleozoic structures of the Frontal Cordillera, but rather of the pattern delineated by the unconformity between the Choiyoi series and the Protero-Paleozoic basement as is interpreted to illustrate the Andean deformation of the Frontal Cordillera basement.

Our maps illustrate precisely the main tectonic features of our study region (Figures 3-5): to the west, a series of north-south trending anticlines and synclines of the WVF that deform the thick Cenozoic and Mesozoic series of the Principal Cordillera, and to the east the succession of east-vergent thrusts of the Aconcagua-FTB. The thrust sheets of the Aconcagua-FTB are thrusted over Neogene intra-mountainous basins and over the basement high of the Frontal Cordillera. Within our northern area, the Paleozoic-Triassic Choiyoi unconformity outlines a broad basement antiformal culmination east of the Aconcagua-FTB (Figure 4). To the south, deformation of the Aconcagua-FTB propagated into the intra-mountainous basins (Figure 5). Our maps appear at first-order remarkably comparable to those of *Ramos et al. (1988) and Ramos et al. (1996b)* for the northern area (Figure 4), and to those of *Thiele et al. (1980) and Giambiagi et al. (2001)* for the southern area (Figure 5). They essentially differ in their higher resolution provided by our large-scale mapping of bedding attitudes from satellite images and aerial photographs, together with DEMs. We also put further emphasis on the geology and structures west of the Aconcagua-FTB on the Chilean side, i.e. within the WVF. Overall, structural styles and units are similar from north to south over our entire study region, further emphasizing a lateral north-south structural continuity (Figure 3-5). Locally, some variations alter this continuity, such as immediately south of the Aconcagua (Argentina) (Figure 4). Such disharmony is attributed to the presence of gypsum, forming locally large diapirs and bulks within the Aconcagua-FTB, as well as in some places to the presence of volcanic edifices such as the Aconcagua or Tupungato volcanoes.

3.2. Building geological cross-sections of the Aconcagua fold-and-thrust belt, with account on the West-Vergent Folds and on the western Frontal Cordillera.

We follow the methodological approach of Riesner et al. (2017) to build our geological cross-sections. We define sections A1-A2 and A3-A4 (Figures 4 and 5 for the northern and southern areas, respectively) perpendicular to the main north-south structural trend. Section A3-A4 is a combination of sections A3-A3' and A4'-A4 so as to avoid non-structural complexities related to magmatic intrusions or to volcanic edifices (Figure 5). The 3D-mapped bedding attitudes (Supplementary Dataset S1 and S2) are taken within 5-35 km wide swaths and projected onto sections A1-A2 and A3-A4. From there, we are able to build a precise sub-surface cross-section over a depth of ~3 km constituted of form-lines derived directly from geological surface observations (i.e. the stratigraphic layers mapped in 3D using satellite images and DEMs), in particular along major river incisions (Figures 4 and 5). An interpretive geometry is then deduced at depth from these direct observations to complete the proposed structural sections (Figures 4 and 5).

Our detailed A1-A2 section (Figure 4b) clearly illustrates all major structural units of our study area, already commented from our map: from west to east (1) the eastern portion of the West Andean-FTB with folded Farellones and Abanico formations, (2) the WVF illustrated by the strongly folded Abanico Formation within the Portillo syncline and the sub-vertical Abanico, Lo Valdés and Río Damas formations, (3) the succession of folds and east-vergent thrust-sheets of the Aconcagua-FTB, and (4) the westernmost Frontal Cordillera forming a large basement antiformal culmination.

The geometry of the eastern part of the West Andean-FTB at this latitude is at first-order comparable with the one already described further south (Riesner et al., 2017), with a large west-verging fold. We do find a slight angular unconformity between the overall conformable Farellones and Abanico formations at the western extremity of section A1-A2 (west of km 5 in section A1-A2 - Figure 4b), indicating that deformation in this area started after deposition of the Abanico formation, but stopped prior to deposition of the Farellones formation. Within the WVF area, we also observe large folds with axial planes dipping ~70°E, even though more symmetric than further south (Figure 5). On the western side of the WVF of section A1-A2, the Farellones formation is conformably folded on top of the Abanico formation implying that the deformation in this area started after deposition of the Farellones formation. It should be recognized however that the relative geometry between Farellones and Abanico Formations over the WVF are defined from very limited outcrops immediately west of the main structures of this unit, and that the observed conformable contact on our northern section only (Figure 4) may be local and apparent. We cannot therefore rule out the possibility of active faulting and folding within the WVF prior or during deposition of the Farellones Formation. To the east of the WVF, deeper Mesozoic units are exhumed and exposed with nearly vertical dip angles, and mark the transition between the west-vergent WVF and the east-vergent Aconcagua-FTB.

The transition between the WVF and the Aconcagua-FTB – and therefore the change in apparent vergence - is marked by a steep thrust fault dipping ~70°W. Within the footwall of this thrust, we observe a large reversed syncline with an almost vertical western flank indicative of an eastward vergence (Figure 4). The Aconcagua-FTB is then characterized by four main east-verging thrusts with ~1-3 km thick thrust sheets (Figure 4). The dip angle of the stratigraphic layers within each thrust sheet decreases eastward from ~30° to ~15°W. At depth, this succession of thrusts is interpreted to root onto a ~2-4 km deep basal décollement within Jurassic gypsum.

Eastward, the frontal Aconcagua-FTB thrust sheets overthrust the syntectonic intra-mountainous Neogene basins, deposited on the thin Mesozoic series conformable over the Pre-Andean basement of the Frontal Cordillera (Figure 4). On the easternmost part of section A1-A2, the geometry of the unconformity between the Permian-Triassic Choiyoi Group over the Paleozoic Gondwana basement outlines the large-scale basement antiform of the Frontal Cordillera (Figure 4b). This broad antiform culmination has a slightly steeper western flank with an axial plane dipping at ~80-85°E. Despite its steep dip angle, such axial plane is averaged over several kilometers and is therefore a robust indication of a large-scale westward vergence.

Similar observations can be made along our southernmost section A3-A4, however they are less well defined due to sparser extractable data from satellite images and due to the complexities related to the presence of Jurassic gypsum (Figure 5). The contact between the Farellones and Abanico formations is not clear as the large La Gloria pluton impedes any precise observation *(Riesner et al., 2017)*. The WVF is characterized by two main west-vergent synclines corresponding to the Quempo and Coironal ranges, with exhumed Mesozoic formations in between. As in the northern area, the transition with the thin Aconcagua-FTB is marked by nearly vertical Mesozoic series thrust over the Aconcagua-FTB along a steep west-dipping thrust. The Aconcagua-FTB is characterized by a series of six east-vergent thrust faults interpreted to root onto a ~2-4 km deep décollement. Deposits of the intra-mountainous Alto Tunuyán basin are involved in two of the easternmost thrust sheets, and are thrust over Mesozoic series conformable over the basement high of the Frontal Cordillera. No continuous observations of the Triassic-Paleozoic Choiyoi unconformity over the westernmost Frontal Cordillera basement were possible along this section to enable 3D mapping of this unconformity.

By restoring our sections using a line-length balancing approach, we find a cumulative shortening of 8-12 km and 6-16 km across the sole Aconcagua-FTB for sections A1-A2 and A3-A4, respectively, and of 10-15 km across the WVF for both sections.

3.3. *Limits on our interpretations, and comparison with previously published cross-sections of the Aconcagua Fold-and-Thrust Belt.*

Our geological and structural sections are built by mapping and projecting 3D bedding attitudes, from DEMs and satellite images. We believe that this approach allows for a precise representation of surface structural geometries averaged over a certain spatial scale, in particular along major river incisions where observations are possible over up to ~3 km high vertical profiles. However, this method relies on the possibility of following continuous layers over a certain spatial scale. Because of the volcanic and volcanoclastic nature of some of the formations, such as the Abanico and Farellones formations within the West Andean-FTB and WVF, or because of the presence of volcanic edifices or gypsum diapirs within the Aconcagua-FTB, some layers may be discontinuous and/or disrupted, and therefore be difficult to map. We estimate that we reduced the associated range of possible values for shortening by integrating the 3D-mapped layers within ~5 to 35 km wide swaths (Figures 4 and 5). We estimate that our mapping and hand-drawn structural reconstruction result in constraining the total shortening with a precision of ~2 to 3 km for the WVF, Aconcagua-FTB and Frontal Cordillera in the case of section A1-A2 and for the WVF in the case of section A3-A4. However, we estimate the range of possible shortening values to be less well resolved, with a precision of ~6-7 km, for the Aconcagua-FTB along section A3-A4 as a result of ubiquitous gypsum diapirs along the Yeso Valley.

Our final cross-sections can be compared to previously published interpretations of the Aconcagua-FTB (Figure 6). Indeed, at the latitude of the Aconcagua (Argentina) – therefore nearby our section A1-A2 - several structural interpretations have already been published *(Ramos, 1998; Cegarra and Ramos, 1996, Rivano et al., 1993)*. Within the Aconcagua-FTB, the structural geometry we propose is clearly similar to the one proposed by *Ramos (1988)* south of the Río Las Cuevas (Figure 6a). We measured a total shortening of ~23 km on the section proposed by *Ramos (1988)*, a value higher than the 8-12 km we obtain here. The main differences between our section and his rely on the details of bedding geometries, in particular in the dip angles of some of the layers and thrust faults, and in the thickness of Jurassic layers. Specific data on the basement paleotopography at depth – and therefore on the thickness of Jurassic series - are non-existent. For simplicity, we propose here a straight and slightly dipping basement surface. This interpretation is not unique and infers a westward thickening of the Jurassic series, leading to thicknesses higher than in the interpretation of Ramos (1988). We believe that the geometry of the subsurface layers is here better defined by our 3D mapping and projection method, by directly following in 3D stratigraphic layers over a certain spatial scale.

On a section north of the Río Las Cuevas, *Cegarra and Ramos (1996)* proposed a different interpretation of the Aconcagua-FTB (Figure 6b), with duplexes at depth, needed in their case to fill missing underlying volumes of rocks in the core of anticlines. As well, most of the WVF are integrated to the Aconcagua-FTB as east-vergent thrust sheets. Such interpretation maximizes the cumulative shortening across the Aconcagua-FTB, with a proposed value of 62.7 km *(Cegarra and Ramos, 1996)*, in the very high range of shortening estimates when compared to other existing interpretations. However, we did not find any evidence of duplexes from field or map observations and propose to interpret the missing rock volumes as related to ubiquitous gypsum diapirs rather than to duplexes. As of the WVF within the area of section A1-A2, our interpretation is totally different from that of *Cegarra and Ramos (1996)* but to the first order similar to the one proposed by *Rivano et al. (1993)* (Figure 6c). Indeed, our data and the observations by *Rivano et al. (1993)* indicate the presence of a large anticline west of Portillo within the Abanico formation followed to the east by a syncline. *Rivano et al. (1993)* propose that these folds are overall symmetrical, in contrast with the westward-vergence deduced here from our detailed and large-scale observations on 3D bedding attitudes. The unconformity between the Abanico and Farellones formations is to the first order similar in our proposed sections and the one from *Rivano et al. (1993)* except for the unconformity located above the anticline west of Portillo. *Rivano et al. (1993)* proposed an important angular unconformity with horizontal stratigraphic layers of the Farellones formation above the anticline west of Portillo, in contrast with the conformably folded geometry of the Abanico and Farellones formations proposed here from our field data and 3D large-scale integrated observations. *Cegarra and Ramos (1996)* section does not show these folds and rather interpret this area as a

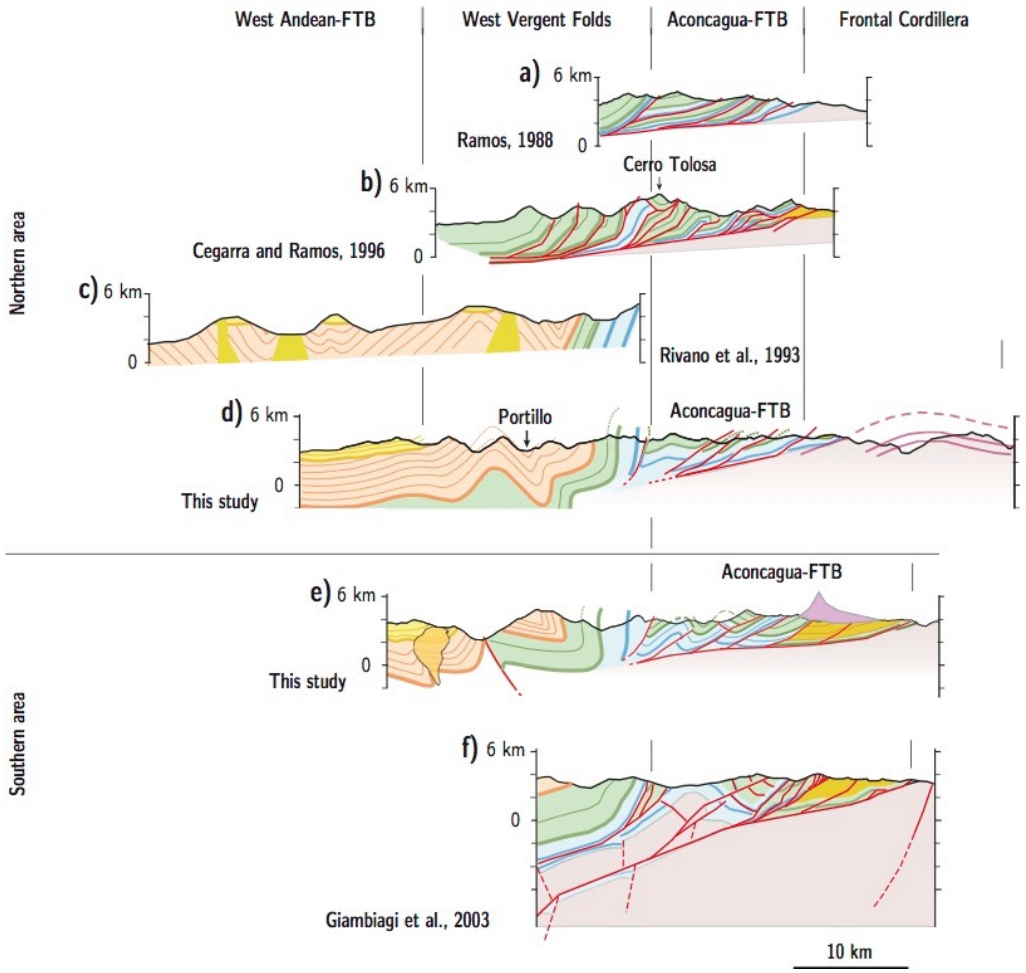

Figure 6 : Compilation of published cross-sections of the West-Vergent Folds and Aconcagua Fold-And-Thrust Belt, compared with our northern (Figure 4) and southern (Figure 5) sections. The published sections have been re-drawn and the colors have been changed for a better comparison between the different studies. FTB : Fold-And-Thrust Belt.

succession of east-verging thrust sheets made of Cretaceous layers, inconsistent with the Oligo-Miocene age of these layers proposed on the Chilean side from field observations and from existing geological maps *(Rivano et al., 1993, SERNAGEOMIN, 2003)*. At least one of these sheets would prolongate eastward as a refolded thrust sheet forming a klippe at the Cerro Tolosa (Figure 6b), thus requiring a minimum displacement of ~15km on this individual thrust *(Cegarra and Ramos, 1996)*. The eastward vergence of these thrusts, as interpreted by *Cegarra and Ramos (1996)*, thus adds many tens of kilometers to the shortening estimated for the Aconcagua-FTB and would imply that most of the structures were built by eastward thrusting on a west-dipping crustal ramp (> 50km of shortening) (Figures 2a and 6b). On the opposite, our own observations suggest a series of tight west-vergent folds, with an overall large-scale top-to-the-west stratigraphic geometry. This interpretation implies that most of the structures are west-vergent. Concerning the Cerro Tolosa "klippe", clear stratigraphic ages for this unit are lacking at this precise location. The geometry of the layers is sub-horizontal, comparable to the unconformable volcanic deposits of the nearby Aconcagua volcano complex. Therefore, we propose a simpler alternative interpretation in which the Cerro Tolosa is a series of discordant volcanic units, composed of Miocene deposits, similar to the nearby Aconcagua volcanics (Figure 4), rather than a klippe of Mesozoic layers. However, this interpretation needs to be verified in the future by precise stratigraphic and dating investigations of the Cerro Tolosa.

Within our southern area (section A3-A4), *Giambiagi and Ramos (2002) and Giambiagi et al (2003)* proposed a section across the Aconcagua-FTB in which the number of thrust sheets slightly differs from ours (Figure 6f). In addition, they propose a large basement-cored anticline (Yeguas Muertas anticline, Figure 5) in

one of the westernmost thrust sheets. The related shortening is therefore maximized with a value of 47 km *(Giambiagi and Ramos, 2002)*, when compared to our estimated shortening of 6-16 km. We did not find any particular field evidence for outcropping basement units in this region nor is it reported on published map *(Thiele, 1980)*. We believe that this interpretation is related to a missing rock volume at depth while building and equilibrating the cross-section. As already proposed in the case of the section by *Cegarra and Ramos (1996)* further north, we interpret the anticlines to be cored by gypsum diapirs, not by imbricated duplexes or basement units. Indeed, along the Yeso valley, gypsum is so ubiquitous that structures and structural geometries may be hardly observable. We therefore prefer a simpler interpretation, in continuity with along strike observations further north (Figures 3 and 6d-e). The section by *Giambiagi et al., (2003)* also suggests shallower westward dip angles for the layers within the WVF, in contrast with our own field and map observations (Figure 6e-f).

Our two sections are comparable in style and cumulative shortening (Figures 4 and 5), and propose a regionally consistent and simple structural interpretation of the Aconcagua-FTB and its surroundings, in contrast with the variety of structural and cumulative shortening interpretations proposed previously (Figure 6). This is consistent with the lateral structural continuity than can be deduced from the structural map of our study region (Figure 3). Together with our precise mapping approach, and 3D projection technique, we are therefore confident in our geological sections and results. We here propose interpretations of the Aconcagua-FTB that appear as the most simple – but regionally consistent – structural solutions satisfying all field and map observations, in particular when compared to previous published interpretations. However, we recognize that our structural interpretation may not be unique in this complex region and that previous interpretations cannot be fully disregarded, at least at this relatively small scale and only considering the Aconcagua-FTB. This will be further discussed in the next sections.

4. Geometry and kinematics of the Principal Cordillera (western flank of the Andes) at 33.5°S.

4.1 Structural geometry of the Principal Cordillera at 33.5°S.

We propose here to synthesize and integrate structural data across the whole western flank of the Andes to upscale our structural reasoning and build a cross-section of the Principal Cordillera within our study region at 33.5°S (Figure 7). The geometry of the West Andean-FTB has been studied in detail by *Riesner et al. (2017)* along section B1-B2 at 33.5°S (Figure 3, 7). Further east, we defined the structural geometries of the WVF, Aconcagua-FTB and western Frontal Cordillera along two sections, A1-A2 and A3-A4 (Figures 4 and 5). Even though section A3-A4 is located in continuity with section B1-B2 and along the final transect we aim at 33.5°S, it is less precise when compared to A1-A2, in terms of geometry of the Aconcagua-FTB or of the western Frontal Cordillera. Because structures show an overall along-strike continuity at large-scale (Figures 3 and 6d-e), we choose to combine the section B1-B2 across the West Andean-FTB from Riesner et al. (2017) with our section A1-A2 across the WVF, Aconcagua-FTB and western Frontal Cordillera to unravel the geometry of the Principal Cordillera at 33.5°S (Figure 7). Matching the details in the structural geometry of the WVF in both regions allows of a proper tying of these two sections.

The West Andean-FTB and Aconcagua-FTB are two units with different structural geometries, aside from their vergence. Indeed, west-vergent folds within the West Andean-FTB were interpreted by *Riesner et al. (2017)* to be related to faults that root at depth into a ~12-15 km deep décollement at the base of the Meso-Cenozoic series. This décollement depth is constrained as such from the Mesozoic series that are exhumed within the WVF, west of the West Andean-FTB. Cumulative shortening across the West Andean-FTB has been proposed to be of ~9-15 km (Riesner et al., 2017). On the other hand, the east-vergent Aconcagua-FTB is composed of thin Mesozoic series deformed over a shallow décollement at ~2 to 4 km depth, with a total cumulative shortening of 8-12 km according to our previous interpretation (Figures 4-6). The Aconcagua-FTB overthrusts the large-scale west-vergent basement antiform culmination of the Frontal Cordillera. Taken altogether, it appears that the east-vergent thin-skinned Aconcagua-FTB is surrounded by larger and deeper west-vergent structural units, with the West Andean-FTB and WVF to the west, and the western Frontal Cordillera to the east (Figure 7). This westward primary vergence is consistent with the overall top-to-the-

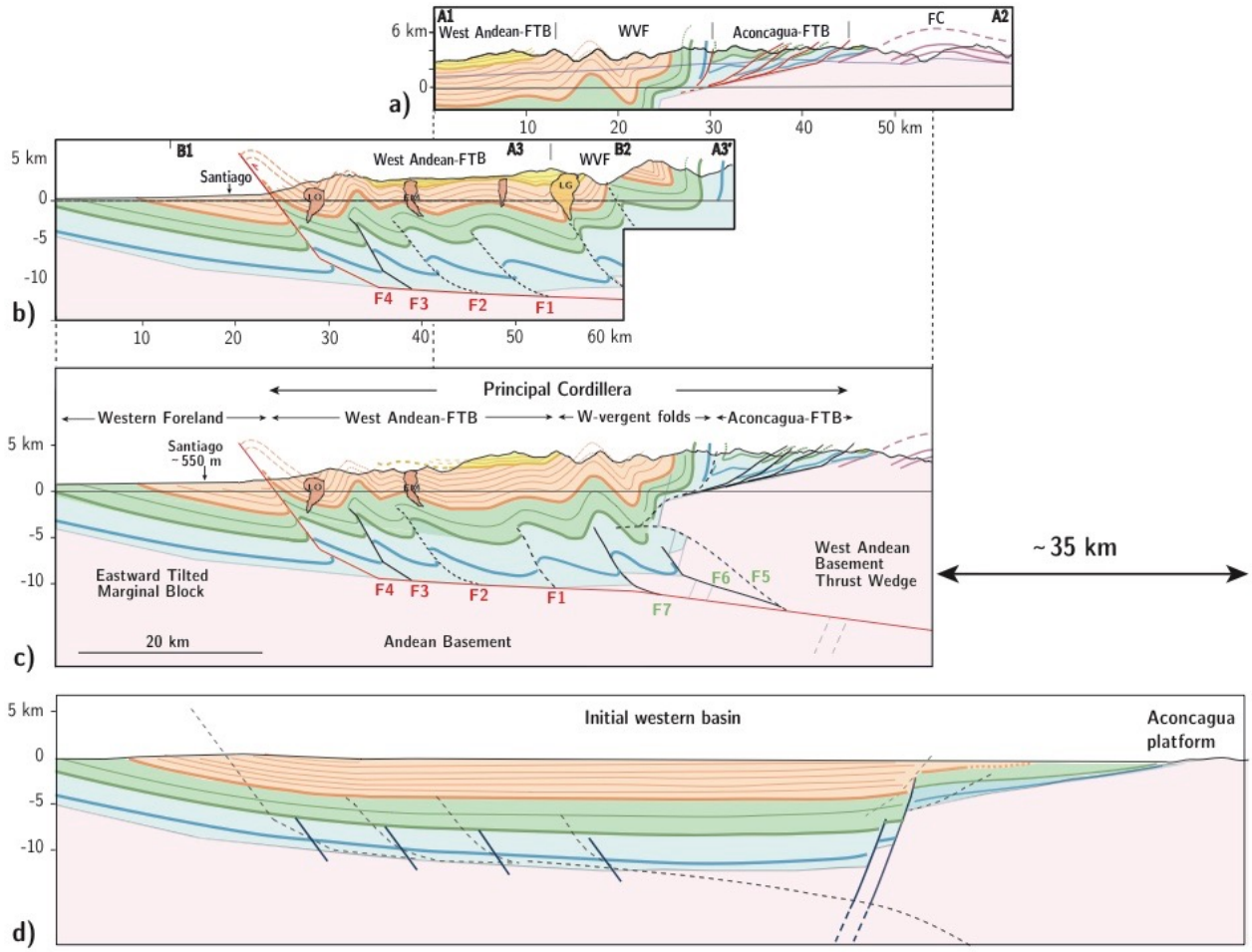

Figure 7 : Synthetic cross-section of the Principal Cordillera at 33.5°S, combining profiles A1-A2 to the east, with B1-B2 to the west. WVF: West-Vergent Folds; FTB: Fold-and-Thrust Belt; FC: Frontal Cordillera; LO: La Obra; EM: El Manzano; LG: La Gloria. a) Subsurface cross-section A1-A2 of the WVF (West-Vergent Folds) and Aconcagua-FTB (Aconcagua Fold-and-Thrust Belt) at ~33°S (Figure 4). b) Subsurface cross-section of the West Andean-FTB (West-Andean Fold-and-Thrust Belt) and WVF at ~33.5°S (B1-B2 section after Riesner et al., 2017, Figure 3, and A3-A3' from this study, Figure 5). Fault labels (F1 to F4) after Riesner et al 2017. c) Interpreted deep geometry of the synthetic cross section across the Principal Cordillera. Faults beneath the WVF labeled F5 to F7 (this study). d) Restored western basin of the Principal Cordillera deduced from the cross-section of figure 7c. Possible inherited normal faults are in dashed blue lines without any drawn displacement due to the lack of constraints. Future faults within the West Andean FTB and Aconcagua FTB are in dashed black lines. A total cumulative shortening of ~35 km is deduced by comparing the section (Figure 7c) and its restored geometry (Figure 7d).

west stratigraphy observed at the regional scale (Figure 3), or in other words with the eastward apparent stratigraphic deepening (in parallel to eastward increasing topography), from Cenozoic series in the west (at low elevations) to Mesozoic series and Paleo-Proterozoic basement in the east (at higher elevations). Given this context, the idea initially proposed by *Armijo et al. (2010)* in which the Aconcagua-FTB is a secondary structural feature within the overall west-vergent Principal Cordillera appears as a reasonable interpretation worth testing using our extensive geological dataset within a kinematic reconstruction.

Figure 7c illustrates our final cross-section of the Principal Cordillera within our study region, by combining the geological evidence presented above. Our results and data however provide further details to properly restore the section and discuss the associated kinematics. The West Andean-FTB and WVF are interpreted as a west-vergent fold-and-thrust belt, with a series of 7 faults (labeled F1 to F7 – Figure 7c) that root onto a ~10-15 km deep décollement at the base of the Mesozoic series *(e.g. Armijo et al 2010, Riesner et al., 2017)*, within a regionally well-known gypsum layer at the base of the Meso-Cenozoic series *(Thiele 1980)*. This décollement needs to connect further east into a basement ramp to allow for the formation of the large-scale west-vergent basement antiform and for the exhumation of the western Frontal Cordillera. Within

this frame, the Aconcagua-FTB is a secondary feature, passively transported on top of the uplifting basement of the Frontal Cordillera. The overall first-order geometry of the Principal Cordillera appears as a large inverted basin, forming a large west-vergent syncline that brings the deep Mesozoic series to the surface within the WVF area (Figure 7c).

Note that we follow the fault labeling of Riesner et al. (2017) for the four most frontal thrust faults of the West Andean-FTB (F1 to F4), and use labels F5 to F7 for the other 3 faults further east. The F0 fault in *Riesner et al. (2017)* is labeled F7 here and is interpreted here as part of the WVF units, based on stratigraphic evidence along section A1-A2 (see section 4.2 below). As explained hereafter, this labeling allows for an easier comparison to the previous work of Riesner et al. (2017) but also follows the kinematic evolution that can be proposed for this western fold-and-thrust belt.

Using a line-length approach on our final section of the Principal Cordillera, we find a total shortening of ~35 km, partitioned as ~9-15 km across the West Andean-FTB - following the results of *Riesner et al. (2017)* -, ~10-15 km across the WVF and ~8-12 km across the Aconcagua-FTB. This implies that the east-vergent structures of the Aconcagua-FTB only accommodate ~30% of the total shortening across the Principal Cordillera whereas the west-vergent units, together the West Andean-FTB and WVF, accommodate the rest. Figure 7d illustrates a possible initial undeformed geometry by restoring our section, with account on the total shortening retrieved from our cross-section. This geometry recalls that already proposed from published paleogeographic reconstructions *(e.g., Mpodozis and Ramos, 1989; Ramos, 1999, 2010)*. The initial asymmetric geometry of the basin is proposed to account for the differences in thickness and sedimentology of the Mesozoic series between the WVF (and subsequently under the West Andean-FTB) and the Aconcagua-FTB. Such asymmetry, with a shallower eastern margin, also allows for a realistic estimate of the exhumation of the Aconcagua-FTB and western Frontal Cordillera. Indeed, in the case of an initially symmetric basin, the Mesozoic series of the Aconcagua-FTB and the basement of the Frontal Cordillera would have been exhumed during Andean deformation from the base of the basin at ~10 km depth, a value too high given sedimentological constraints and the absence of metamorphism within the Aconcagua-FTB *(Lo Forte, 1992 cited in Ramos et al., 1996a, Aguirre-Urreta, 1996, Aguirre Urreta and Alvarez, 1998, cited in Giambiagi et al. 2003b)*. A simple geometry is proposed for the deeper basin on the western side in the absence of any evidence for particular complexities, even though we cannot discard their existence.

4.2 Constraints on the timing of deformation across the Principal Cordillera.

To incrementally reconstruct our cross-section from the restored initial asymmetric basin, we here first synthesize chronological constraints on the timing of deformation of the different structural units. In the case of the faults labeled F1 to F4 within the West Andean-FTB, the timing was constrained in detail in *Riesner et al. (2017)*. The timing of deformation on these different faults is defined relative to deposition of the Abanico and Farellones formations, as inferred from mapped - either unconformable or conformable - contacts between them, all along the West Andean-FTB. This unit has been interpreted as a classical forward (here westward) propagation of thrusts, which initiated by ~20-25 Ma, prior to deposition of the Farellones formation.

Within the WVF, the Farellones formation is mostly absent, either because it has never been deposited or because it has been since eroded away. Some layers are however slightly preserved on the western flank of the anticline west of Portillo (Figure 4) associated to the F7 fault (Figure 7). There, the Farellones and Abanico formations appear conformably folded, suggesting that deformation associated to F7 started after deposition of both these formations. The lateral continuity of the contact between Abanico and Farellones formations, from the West Andean FTB to the WVF, suggests the existence of a hiatus between these two formations, at least within the WVF. We interpret here the conformity between these two formations as an indicator that deformation on F7 started well after initiation of deformation within the West Andean-FTB, as an out-of-sequence fault. No particular constraints were retrieved from field and mapping observations for the timing of the other F5 and F6 faults of the WVF. However, we acknowledge that the conformable contact between the Farellones and Abanico Formations over fault F7 may be local and apparent, given the limited observations and the presence of a hiatus between the two formations. We therefore cannot discard the possibility for an

unconformity between the two formations over the WVF that has been since eroded away. However, because thermochronological data suggest that exhumation within the WVF was overall ongoing by ~13 to ~5 Ma *(Fock et al. 2005, 2006)*, we propose to consider that faults F5, F6 and F7 of the WVF have been out-of-sequence and that they have been active coevally with westward in-sequence deformation of the West Andean-FTB, probably coeval with F3 and/or F4.

Chronological constraints on thrusting across the Aconcagua-FTB can be retrieved from the overthrusted syntectonic intra-mountainous basins and from the syntectonic deposition of Aconcagua-related volcanics on top of the Aconcagua-FTB thrust sheets. Within the Alto Tunuyan basin, along our southern section and ~50-100 km south of our synthetic section (Figure 3), an age of 18.3 Ma from a volcanic rock of the Contreras formation below the syntectonic Neogene strata provides a maximum age for the basin *(Giambiagi et al., 2000)*. An age of 16-17 Ma is attributed to the base of the syntectonic deposits by *Giambiagi et al. (2014)*, while new U-Pb ages on zircon appear to constrain the depositional time span mainly between ~15 and ~9 Ma, and perhaps as young as ~6 Ma *(Porras et al., 2016)*. Because these intra-mountainous basins are accreted to, and overthrust by the Aconcagua-FTB, this suggests that deformation of the Aconcagua-FTB started at least by ~17-15 Ma. In the southern part of the Alto Tunuyan basin, an age of 5.9 Ma *(as reported by Giambiagi et al., 2001 and Giambiagi and Ramos, 2002)* for andesites unconformable on top of the syntectonic deposits implies that Aconcagua-FTB deformation stopped before the end of the Miocene. Further north, the Miocene Aconcagua volcanic deposits ontop the Aconcagua-FTB thrust sheets show patterns of syntectonic deformation. Indeed, basal deposits appear slightly folded, while topmost deposits are essentially undeformed *(Ramos, 1985 cited in Godoy, 1988 and Ramos et al., 1996c)*. The top of the folded volcanics was dated to 11.3 ± 0.5Ma at an altitude of ~5200 m *(Ramos, 1985 cited in Godoy, 1988 and Ramos et al., 1996c)*, and topmost – unfolded - volcanics were dated to 9.63 ± 0.44 Ma *(Godoy et al., 1988)*. These observations and ages imply that deformation of the Aconcagua-FTB in the Aconcagua region occurred mostly before ~11 Ma and stopped before ~9.5 Ma.

In the case of the Frontal Cordillera, recently published thermochronological data place important constraints on the timing of exhumation of the large-scale basement culmination. From (U-Th)/He ages on apatites within the Choiyoi Group of basement units, *Hoke et al (2014)* proposed that exhumation of the Frontal Cordillera initiated by ~25 Ma, concomitant to deformation of the Aconcagua-FTB. This also suggests that exhumation of the Frontal Cordillera basement initiated by the time deformation initiated across the West Andean-FTB, according to published chronological constraints on the deformation of this unit *(Riesner et al., 2017)*. Following *Hoke et al. (2014)*, this timing for initial uplift and exhumation of the Frontal Cordillera is earlier than previously proposed, and, even though not emphasized by the authors in the source paper *(Hoke et al 2014)*, this early initiation of exhumation of the Frontal Cordillera is difficult to reconcile with the east-vergence conceptual models of evolution of the Central Andes (Figure 2 – section 2.3). Recently published U-Pb analyses of inherited zircons from the Alto Tunuyan intra-mountainous basin are compatible with exhumation of the basement of the Frontal Cordillera already by ~15 Ma *(Porras et al., 2016)*, a result that would be compatible with an early uplift of the Frontal Cordillera. All these findings suggest that the Frontal Cordillera has been exhuming since the Early Miocene and not buried beneath eastern foreland sedimentation *(Hoke et al., 2014; Riesner 2017)*.

4.3 Kinematic evolution of the western flank of the Andes at 33.5°S.

Combining these chronological constraints with geological observations and inferences on the shortening and on the style of deformation, we reconstruct the kinematic evolution of the Principal Cordillera within our study region at 33.5°S latitude (Figure 8). Such incremental reconstruction allows for testing the viability of our cross-section (Figure 7) and of the proposed initial asymmetric basin. We propose a kinematic model of incremental deformation of the Principal Cordillera through 7 temporal snapshots, according to the above-mentioned chronological constraints:

- *Time 1, Late Oligocene (before ~25 Ma)*: the initial Meso-Cenozoic basin is not yet affected by Andean compressional deformation and is being filled with volcanic and volcano-clastic rocks (Abanico Formation).

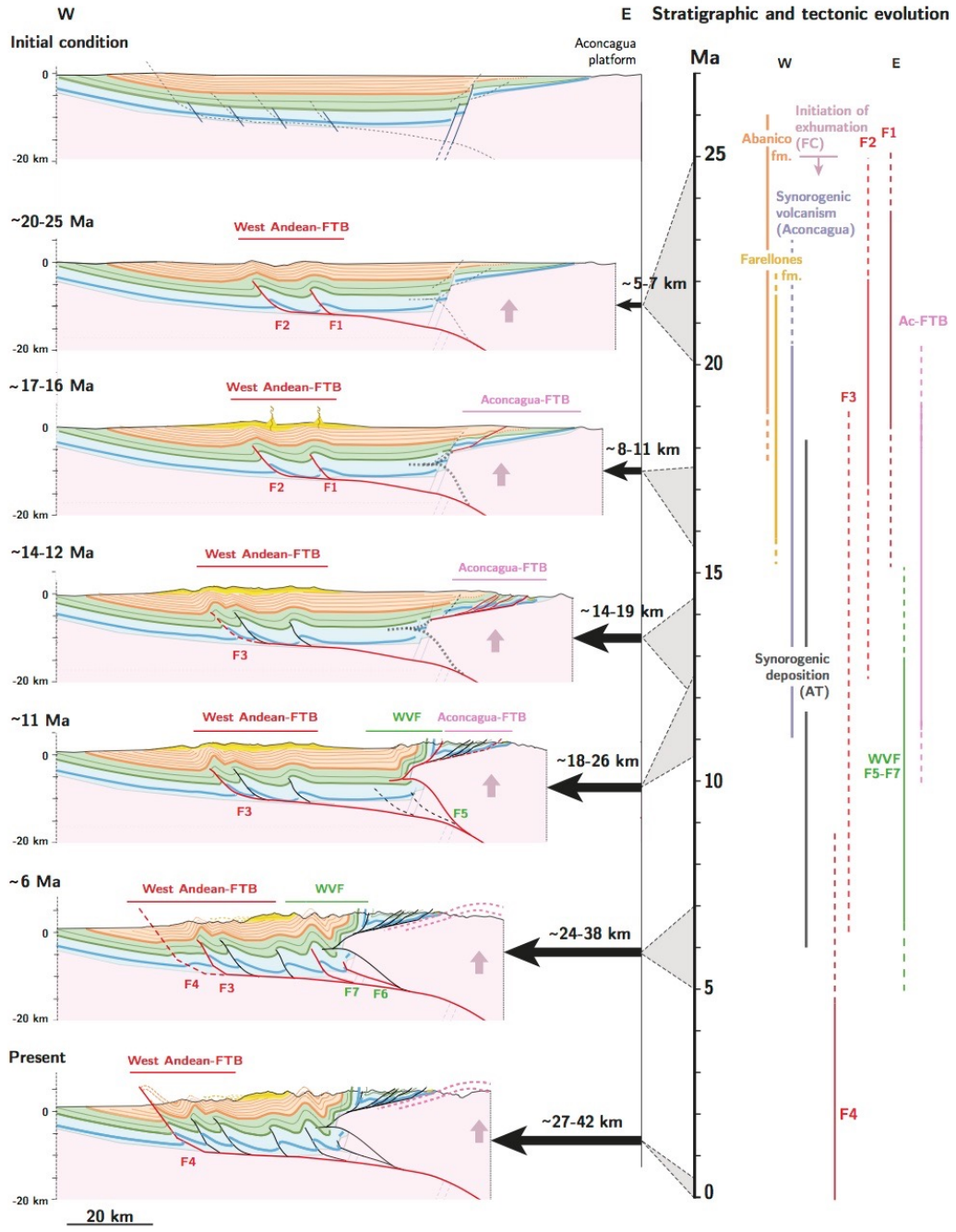

Figure 8 : (left) Kinematic evolution of the Principal Cordillera. (right) Synthesis of chronological constraints, as deduced from angular unconformities between Farellones and Abanico formations, and as derived from age constraints and provenance studies on the synorogenic Neogene intra-mountainous basins (AT : Alto Tunuyan Basins), on the Aconcagua volcanic complex, and of thermochronological studies on the Frontal Cordillera (see text for further discussion). Total cumulative shortening is determined at each time step. Thrust faults are reported in red when active during each period of incremental deformation. Inactive faults are indicated in black. Volcanic edifices feeding Farellones series have been schematized at stage 17-16 Ma. FTB: Fold-And-Thrust Belt; WVF: West-Vergent Folds; Ac-FTB: Aconcagua Fold-And-Thrust Belt. Faults F1 to F4 after *Riesner et al. 2017*. Faults F5 to F7 further detailed in main text.

- *Time 2, Early Miocene (~20-25 Ma)*: deformation has started within the initial basin, with the propagation of the F1 and F2 faults of the West Andean-FTB (Riesner et al, 2017). Exhumation of the Frontal Cordillera basement initiates *(Hoke et al, 2014; Riesner, 2017)*.

- *Time 3, Late Early Miocene (~17-16 Ma)*: the Farellones Formation is being deposited while deformation on F1 and F2 keeps ongoing. The contact between Farellones and Abanico Formations is therefore erosive with an angular unconformity above F1 and F2, but is rather a hiatus slightly further east (future location of F7).

Also, it should be noted that deposition of the volcanic and volcano-clastic Farellones formation occurs nearby former volcanic edifices, independently of the existing topography. The Aconcagua-FTB starts deforming as the basement of the Frontal Cordillera is prograding westward and being uplifted.
- *Time 4, Early Middle Miocene (~14-12 Ma)*: deposition of the volcanic Farellones Formation ends, while deformation propagates onto fault F3 of the West Andean-FTB. Further east, deformation of the Aconcagua-FTB proceeds with an eastward in-sequence propagation of thrust sheets over the uplifting basement of the Frontal Cordillera.
- *Time 5: Late Middle Miocene (~11 Ma)*: deformation continues on F3 (West Andean-FTB). Out-of-sequence deformation initiates within the WVF, within a triangular zone at the forefront of the uplifting basement. Exhumation of the eastern WVF proceeds *(Fock et al., 2005, 2006)* as the Mesozoic series of the Lo Valdés and Río Damas formations verticalize west of the Aconcagua-FTB. The triangular zone disconnects the Aconcagua-FTB décollement from the rest of the deforming basin, precluding further deformation on the Aconcagua-FTB.
- *Time 6, Late Miocene (~6 Ma)*: out-of-sequence deformation proceeds within the WVF with deformation on F6 and F7, before probably ending. Deformation on F3 gets to an end, before propagating onto F4 (West Andean-FTB). Exhumation of the large-scale basement antiform of the Frontal Cordillera keeps ongoing.
- *Time 7 Present*: uplift of the Frontal Cordillera keeps ongoing above the basement ramp that reaches the surface further west at the level of fault F4 (West Andean-FTB), ie. at the level of the seismically active San Ramón fault east of Santiago de Chile *(Armijo et al 2010; Vargas et al., 2014, Riesner et al., 2017)*. The final cumulative shortening across the Principal Cordillera reaches a value of ~27-42km.
Or reconstruction proposes a viable kinematic solution for the evolution of the Western Andes at the latitude of Santiago (Chile) and of the Aconcagua (Argentina) that reconciles existing structural and chronological constraints.

5. Discussion

5.1 Limits on our kinematic reconstruction of the Principal Cordillera.

Despite some local uncertainties related to the difficulty of following discontinuous volcanic layers or to the presence of gypsum and volcanoes, our approach enables us to image precisely the subsurface geometry of the stratigraphic layers, in particular along major river incisions. We estimate the precision of the total shortening estimate related to our detailed 3D mapping to be of ~2-3 km. The final precision in total shortening is however larger, in particular because of the poorly resolved geometry of the initial basin. The thickness of the Cenozoic to Mesozoic formations located within the eastern West Andean-FTB and the WVF imply an initial undeformed ~15 km deep Andean basin. Furthermore, petrological analysis of the WVF Abanico, Lo Valdes and Río Damas formations revealed the presence of low-grade sub-greenschist metamorphic minerals, implying a burial depth of 5.5 km for the Abanico series and 7.5-15 km depth for the Río Damas and Lo Valdes Formations *(Robinson et al, 2004)*. Given this, we tested the possibility of an initially symmetric ~10-15 km deep undeformed basin. However, this initial geometry implies a ~15-20 km exhumation on the Aconcagua-FTB, at odds with existing sedimentological constraints on the Mesozoic series of the Aconcagua-FTB *(Lo Forte, 1992 cited in Ramos et al., 1996a, Aguirre-Urreta, 1996, Aguirre Urreta and Alvarez, 1998, cited in Giambiagi et al. 2003b)*. To minimize exhumation of the Aconcagua-FTB and to account for the initial sedimentation of the Mesozoic series within a shallow platform, an asymmetric basin with a west-dipping normal fault system on the eastern side of the basin has been chosen (Figure 7d). However, the geometry of these faults and of the structural step between the base of the basin and the Aconcagua-FTB platform is not known in detail. We estimate that the uncertainty related to this unknown widens by ~3-4 km the precision on our total shortening estimate. To be conservative, we therefore evaluated the precision on our total shortening estimate to ~6 km.
Additional limits on our kinematic reconstruction of the evolution of the Principal Cordillera derive from chronological constraints. In the case of the evolution of the West Andean-FTB, these are related to the resolution on the precise ages of the Farellones and Abanico formations, as well as to the quality of the

observations on their relative deformation. For further details on these, we refer to the discussion of *Riesner et al. (2017)*. Following the same approach, and based on the absence of an angular unconformity between these two formations, we propose that faults beneath the WVF are out-of-sequence. However, this inference relies only on one single local observation west of Portillo (Figure 4) that applies solely to fault F7 along our northern section, and that has been extended to faults F5 and F6 in our reconstruction. Because thermochronological data within the WVF of our southern section above F7 indicate that exhumation was ongoing by ~13 to 5 Ma *(Fock et al, 2005, 2006)*, we believe that considering the WVF as an out-of-sequence structural ensemble over all our study area is a reasonable hypothesis. The timing that can be proposed from this limited constraint on the deformation within the WVF is however consistent with the ending of deformation across the Aconcagua-FTB (Figure 8).

In our reconstruction, we considered all age constraints for initiation and ending of deformation of the various tectonic units of the Principal Cordillera (West Andean FTB, WVF and Aconcagua FTB), taken wherever available along our southern and northern sections. However, despite the clear lateral structural continuity within our study region (Figure 3), we cannot discard the possibility of diachronic deformation along strike, which would be difficult to constrain with existing age data. However, a diachronicity of a few Myr would not impact much our kinematic reconstruction to the first order (Figure 8), and should be considered as the temporal resolution of the proposed evolution of the Principal Cordillera. Thorough age constraints and geometric observations would be needed to further explore any lateral diachronicity, and are beyond the scope of this paper.

Given these uncertainties in the timing of deformation and in the cumulative shortening, we believe our kinematic reconstruction of the Principal Cordillera to be robust. Indeed, the proposed kinematics imply that exhumation of the Frontal Cordillera basement initiated together with deformation inception within the West Andean-FTB (Figure 8), which is confirmed by independent published data *(Hoke et al., 2014)* as well as our own preliminary thermochronological results *(Riesner, 2017)*.

5.2 Deformation style and structural inheritance within the Principal Cordillera at 33.5°S: comparison to the Western European Alps.

Based on available constraints on the sedimentology and thickness of Mesozoic series of the WVF and Aconcagua-FTB, and on their later exhumation, we propose that the initial western basin of the Principal Cordillera was asymmetric, with a large deep half-basin separated from a shallow platform to the east by west-dipping normal faults. This is based on studies suggesting the existence of a paleogeographic high for the Aconcagua area composed of sediments characteristic of shallow platform environments *(Groeber, 1918; Aguirre-Urreta, 1996, Aguirre Urreta and Alvarez, 1998 cited in Giambiagi et al. 2003,* Figure 7*)*. Possible inherited normal faults have been schematically drawn in the western deep part of the basin, solely for illustration due to the lack of constraints on these potential faults. Such initial geometry and the mechanical contrast between the proposed deep basin and shallow platform may have played a role in localizing deformation. As has been proposed elsewhere *(e.g. Bellahsen et al., 2012; Lafosse et al., 2016)*, the inferred initial normal faults separating the basin and the platform have not been inverted into reverse faults, with a vergence towards the platform, probably as a consequence of the mechanically non-favorable high fault dip angle. To the contrary, the initial horst basement high to the east forms the mechanical backstop of the fold-and-thrust belt propagating into the sedimentary layers of the initial half-graben (Figure 8). Localization of the successive outward propagating faults may be controlled either by the mechanical properties of the layers that operate as décollements or by the presence of east-dipping secondary normal faults within the deep basin (Figure 7).

In addition to localizing Andean deformation to the west of the initial basement culmination, favorable décollement levels within the basin such as Jurassic evaporites may have played a role in controlling the kinematics of deformation during Andean orogeny. As already noted by *Riesner et al. (2017)*, Jurassic gypsum has been reported to the east of the initial basin of the Principal Cordillera, within the WVF and the Aconcagua-FTB *(Thiele, 1980; Armijo et al., 2010)*, but is inexistent further west within the Mesozoic series

of the Coastal Cordillera. The westward progressive disappearance of such favorable décollement level within the deep basin has been proposed to be possibly responsible for the westward decrease in the fold wavelengths of the West Andean-FTB (associated to F3 and F4, Figures 7-8) as well as for the surface emergence of the sole most frontal fault (San Ramón fault F4, Figures 7-8) *(Riesner et al., 2017)*. Out-of-sequence faulting on F5-F7 beneath the WVF seems coeval with thrusting on the most frontal faults of the West Andean-FTB (F3 and F4), and may therefore also be due to the westward fading of Jurassic evaporites. This is comparable to the sandbox experiments of *Nieuwland et al. (2000)* in which a change in the fold-and-thrust belt décollement from low to high basal friction favors out-of-sequence thrusting. Furthermore, the presence of a basement step on the décollement level, at the front of the fold-and-thrust belt can result in the formation of a long thrust sheet required to allow for outward propagation of deformation *(Nieuwland et al., 2000; Nieuwland et al. 2001; Bellahsen et al., 2012)*. In this case, out-of sequence thrusting is necessary to recover critical taper. Thus, the spatial distribution of Jurassic evaporites and the inherited steps along the décollement layer may control out-of-sequence faulting beneath the WVF.

In our kinematic reconstruction, outward propagation of deformation into the initial basin is coeval with the uplift of the large-scale basement antiform of the Frontal Cordillera (Figure 8). This uplift is sustained by a deep ramp that connects to the décollement beneath the West Andean-FTB. While uplifted, the Frontal Cordillera basement antiform is also overthrusted passively by the eastward Aconcagua-FTB. The implied basement geometry and kinematics is that of a crustal scale triangular zone, similar – even though at a larger crustal scale - to passive-roof thrust sheets observed in some foreland basins *(Bonini, 2001)*. Analogue models suggest that such passive-roof thrust sheets may be favored in the case of low friction/ductile décollement levels and/or in response to syntectonic sedimentation *(Bonini, 2001)*. In our case, it is probable that the syntectonic deposition of the Farellones formation atop the deforming West Andean-FTB favored the passive transport of the Aconcagua-FTB over the Frontal Cordillera basement. Such interactions between tectonics and surface processes have already been invoked for the particular case of the outward deformation of the West Andean-FTB *(Riesner et al., 2017)*. In addition, the ubiquitous presence of Jurassic gypsum within the Aconcagua-FTB provides a favorable low-friction ductile décollement level to favor the passive-roof transport of the Aconcagua-FTB over the uplifting Frontal Cordillera. Outward propagation of deformation and passive-roof transport above a basement backstop coexist and are coeval in our case study, comparable to smaller scale structures observed elsewhere in foreland basins *(Davis and Engelder, 1985; Gwinn 1963)*. This coexistence is in our case only disrupted by the late out-of-sequence deformation of the WVF that we relate to the possible westward changes in the mechanical properties of the basal décollement.

The kinematics of the western flank of the Andes seems therefore primarily controlled by the mechanical properties of the sedimentary layers inherited from the initial western basin of the Principal Cordillera, in particular by the existence (or not) of abundant Jurassic gypsum layers, and to some extent to potential interactions between outward deformation propagation and syntectonic Farellones deposition. The Aconcagua-FTB is a particular structural feature that is only observed over ~250 km along-strike within Central Chile and that no longer exists with such geometry north of ~32°S. The along-strike existence (or not) of such east-vergent thin-skinned fold-and-thrust belt passively transported over an uplifting large-scale basement antiform could be related to the presence (or not) of gypsum within the initial basin, as well as to the structure of this basin. As such, the along-strike structural variations within the Principal Cordillera could be related to – and therefore be indicative of – variations in the initial paleogeography and associated structures.

Finally, the geometry and kinematics we propose for the Principal Cordillera as well as the initial asymmetric basin are comparable to those proposed in another context for the Western European Alps across the Vercors – Oisans section *(Bellahsen et al., 2012)* (Figure 9). There, an initial asymmetric basin in a passive margin context (Grenoble Basin), with west-dipping normal faults on its eastern flank is proposed. These normal faults have not been inverted into thrust faults during basin inversion. Instead the initial Belledonne basement high forms the backstop of the Vercors fold-and thrust belt propagating outward within the initial basin with a basal décollement localized within the marly Liassic. The existence of such low friction décollement, as well as the initial geometry of the basin, allowed for a back-thrust rooting into these marls and passively thrusted over the uplifting Belledonne massif *(Deville et al., 1994, Bellahsen et al., 2012)*. Such kinematics and structural geometry imply a crustal-scale triangular zone for the uplifting and prograding basement,

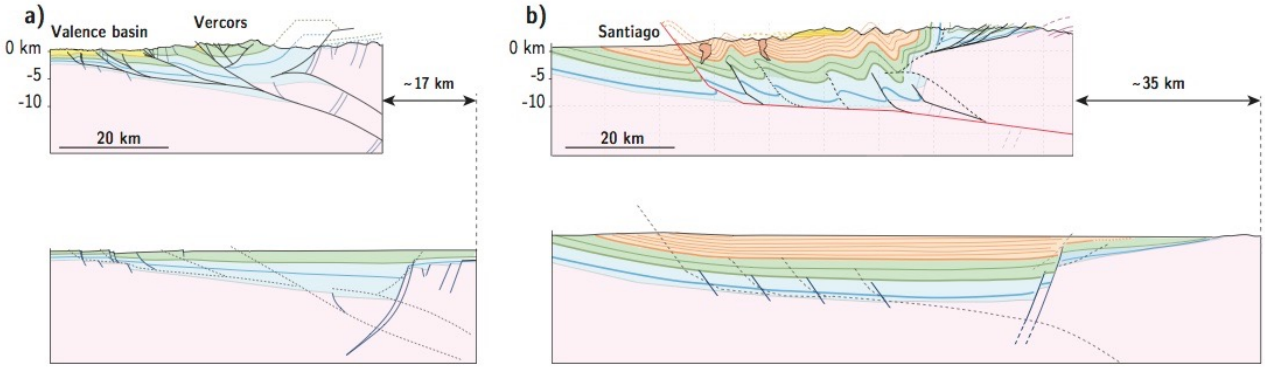

Figure 9 : Comparison of frontal orogenic deformation in (a) the Western European Alps taken here as a model of collision-type mountain belt (figure redrawn from *Bellahsen et al., 2012* - colors have been changed for better comparison), and (b) the western Andes at 33.5°S (This study) considered here as the case-example of a subduction-type belt. Section of the Western European Alps at the level of the Vercors-Oisans.

comparable to our results on the Andean Principal Cordillera of Central Chile at 33.5°S (Figure 9). As also indicated here for the Andean case, along-strike structural variations have been reported within the Western European Alps *(Bellahsen et al., 2014)*: passive back-thrusting over the uplifting basement is not observed everywhere, and no longer exists further north along the Bornes-Mont Blanc section. Such lateral structural variations can also be attributed to variations in the initial paleogeography and deposition within the pre-Alpine basins. It is important to note the differences in dimensions of the initial Alpine and Andean basins, with larger and deeper deposition in the Andean case (Figure 9). Such differences may indeed imply different thermal and mechanical initial conditions. We also note that all alpine-type fold-and-thrust belts have basement culminations in their hinterland acting as backstops and exhumed coevally with the foreward thrusts *(e.g., Boyer and Elliott, 1982; Malavieille, 1984; McClay and Whitehouse, 2004; Leloup et al., 2005; Lacombe and Bellahsen, 2016)*, an observation which clearly recalls our Andean kinematic model (Figure 8).

5.3 Crustal-scale cross-section of the Andes at latitude 33.5°S,

5.3.1 Building a crustal-scale section of the Andes at 33.5°S

Our cross-section of the Principal Cordillera (Figure 7) is completed along its eastern flank using published sections within the Cuyo basin and the Frontal Cordillera at 33.5°S (Section B3-B4, Figure 3) (*Garcia et al., 2005; Giambiagi 2014; Giambiagi et al., 2015)*, and at depth using geophysical constraints on Moho depths from receiver functions *(Gilbert et a., 2006; Gans et al., 2011)* to build a crustal-scale section of the Andes within our study region (Figure 10).

Published shortening estimates on the eastern front of the Frontal Cordillera are variable. Ramos et al., 1996a proposed that the shortening of the belt was mostly restricted to the Principal Cordillera as the Frontal Cordillera uplifted as a rigid block. However, more recent estimations suggest about ~18 km *(Ramos et al., 2004)* and 16 km *(Giambiagi et al., 2014)* of shortening across the Frontal Cordillera and its foreland. At 33.5°S, the currently active eastern front of the Frontal Cordillera does not show any evidence of an important east-vergent thrust and appears similar to passive mountain fronts with relatively limited deformation. However, to the North, at 33°S, the presence of an eastward thrust, the El Salto-La Aguadita fault, is clearly visible in the field as described by *Garcia and Casa (2014)*. Thus, even though non-observable in the field, blind frontal thrusts may exist further south at 33.5°S latitude. *Giambiagi et al. (2014)* proposed 16 km of shortening across both the Frontal Cordillera and the eastern foreland, but without providing the detail of its partitioning between the Frontal Cordillera, its eastern front and the Cuyo basin. In *Giambiagi et al. (2015)* and *Garcia and Casa (2014)*, the shortening across the Cuyo basin at this latitude is estimated to ~2-4 km.

Thus, we infer that the remaining ~12-14 km of the bulk shortening would be accommodated by eastward deformation of the Frontal Cordillera, and, according to Figure 5 of *Giambiagi et al. (2014)*, specifically at the eastern front of the Frontal Cordillera. Without any additional discussion and geological constraint provided by *Giambiagi et al. (2014)*, we suppose that large thrusting at the eastern front is required in their model to exhume the Frontal Cordillera to its current altitude during the last ~10 Myr. Based on our field observations, the eastern front seems to have accommodated little deformation and, even though difficult to estimate, we propose a relatively limited cumulative deformation on this mountain front of no more than ~1-5 km of shortening. We favor the initial interpretation of *Ramos et al. (1996)* of a basement uplifting as a rather rigid block. We add ~1-4 km of shortening to account for large-scale folding of the broad Frontal Cordillera anticlinorium. We consider that exhumation of the Frontal Cordillera started ~20-25 Myr ago *(Hoke et al., 2014; Riesner, 2017)*. Given all these limitations, we integrate the structural section *(Giambiagi et al., 2014)* and shortening estimate in the Cuyo basin from Garcia and Casa (2014) and *Giambiagi et al. (2015)* (Section B3-B4 in Figure 3) to build the section of the entire Andes shown in Figure 10.

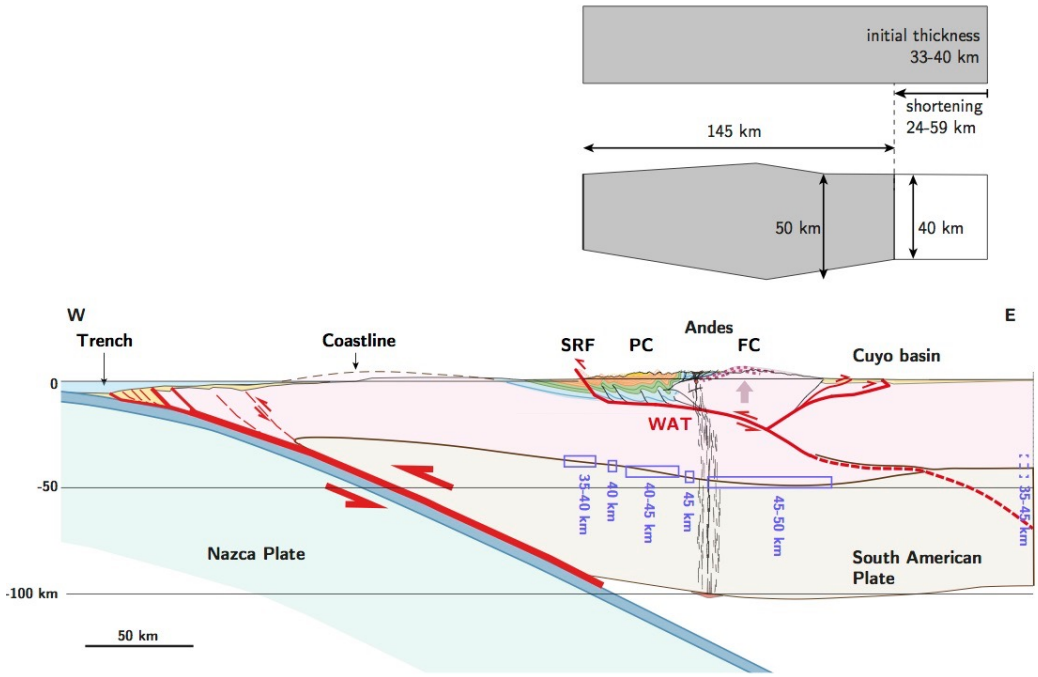

Figure 10 : Lithospheric-scale cross-section at ~33.5°S (location on Figure 1), derived by combining our cross-section of the Principal Cordillera (PC) (Figure 7) with published cross-sections of the eastern Andean front (Section B3-B4 in Figure 3, inspired from Giambiagi et al., 2014), as well as existing geophysical constraints on Moho geometries (Gans et al., 2011) (blue rectangles). SRF : San Ramón Fault ; FC : Frontal Cordillera. The overall geometry of the crustal orogenic wedge is used in a crustal-scale mass balance approach to derive cumulative shortening (top right), independently of the structural interpretation of the mountain range.

At depth, crustal thickening beneath the Andes is derived from existing geophysical constraints on the Moho geometry. At the latitude of our study region (33.5°S), a maximum crustal thickness of ~50-60 km beneath the topographic high of the Andes has been deduced from gravity modeling *(Introcaso et al., 1992; Tassara et al., 2006)* and seismological data *(Fromm et al., 2004; Gilbert et al., 2006; Alvarado et al., 2007)*. More recently, *Gans et al. (2011)*, imaged the Moho at 29-34°S latitude using broadband data and receiver functions. At 33.5°S, they estimated a Moho depth of 30-40 km under the Central Depression, of 40-45 km under the Principal Cordillera and of 45-50 km under the Frontal Cordillera (Figure 10).

Figure 10 illustrates our final crustal-scale cross-section, built by combining our structural data on the Principal Cordillera (Figure 7), together with data on the eastern Andean front and on Moho depths. The larger dimensions and cumulative shortening, as well as the longer-lasting west-vergent deformation of the Principal

Cordillera appear indeed dominant when compared to east-vergent deformation of the Aconcagua-FTB or of the Cuyo Basin and eastern Frontal Cordillera thrusts. Taking all these data and considerations together, we therefore propose a westward crustal-scale thrusting of the Frontal Cordillera over the basement of the Central Depression, synthetic to the subduction zone further west in a bi-vergent belt with both the western and eastern fronts presently active. The sub-surface observations and interpretations on structures and kinematics are consistent with Andean crustal thickening as defined at depth from geophysics (Figure 10), even though geophysical data have not been initially interpreted within this perspective.

5.3.2 Crustal shortening across the Andes at ~33.5° S.

Our final crustal-scale cross-section of the Andes at ~ 33.5 °S (Figure 10 - see location on Figure 1) suggests a total shortening of ~31-55 km retrieved when summing up the contribution of each tectonic unit previously discussed in detail. This is roughly compatible with, or little less than, previously published estimates on bulk Andean shortening derived from cross-sections around 33.5°S: 35-50 km *(Armijo et al., 2010)*, 55km *(Giambiagi et al., 2012)*, ~70 km *(Giambiagi and Ramos, 2002; Giambiagi et al., 2014)*. Our final structural interpretation appears similar to the first order to that of *Armijo et al. (2010)* in terms of overall kinematics. We do however emphasize that we reached this interpretation from a thorough independent quantitative description and discussion of geometries and chronology of deformation for all tectonic units forming the Andes at this latitude. Second-order differences in structures and total shortening between our section and that of *Armijo et al (2010)* result from our refined geometry of the Principal Cordillera as deduced from *Riesner et al. (2017)* for the West Andean-FTB and from this study for the WVF, Aconcagua-FTB and Frontal Cordillera. On the other hand, our crustal-scale interpretation and associated crustal shortening is significantly different from those proposed by *Giambiagi et al. (2014)*. Indeed, most of their shortening values are in the upper part of - or above - the range of values proposed in our model. They propose a model accommodating 52 km of shortening across the Principal Cordillera and 16-18 km across the eastern foreland and Cuyo basin, in contrast with our findings of ~27-42 km of shortening across the Principal Cordillera and ~4-13 km on the Frontal Cordillera and Eastern foreland. As already discussed, we infer that the intense deformation proposed by *Giambiagi et al. (2014)* at the eastern front is a model requirement to exhume the Frontal Cordillera by east-verging thrusting over the last ~10 Myr. Within the Principal Cordillera, the additional difference between our results and the structural model of *Giambiagi et al. (2014)* relies on the different interpretations of the WVF area. Indeed, *Giambiagi et al. (2014)* propose that the Principal Cordillera absorbed 17 km of shortening "at its western slope" (thus likely associated with westward deformation), and 35 km of eastward shortening on the Aconcagua-FTB including the WVF, at odds with field observations, as discussed in section 3.3.

Crustal shortening can be estimated independently from any structural model by considering a crustal-scale area balance. Mass and surface conservation implies that crustal shortening is compensated by crustal thickening (Figure 10). Here, we neglect mass removal by surface erosion as finite exhumation is not significant in the Central Andes *(Hoke et al., 2014; Robinson et al., 2004; Riesner, 2017)*. We consider an initial undeformed crustal thickness of 33 to 40 km. These values are derived from Moho depths inferred from broadband data and receiver functions under the undeformed Cuyo basin ~150 km east of the Andean front, but ~100 km north of our section *(Gans et al. 2011)*. Maximum Moho depths are presently of 50 km beneath the high topography of the Andes *(Gans et al. 2011)* (Figure 10). The width of the orogen is taken as ~145 km, from the San Ramón fault to the eastern deformation front within the Cuyo basin. Given the rough geometry of the deformed Andean crustal wedge and our estimate of possible initial crustal thickness, we obtain an average total crustal shortening of ~24 to 59 km across the entire Andes at 33.5°S latitude. The crustal shortening of ~31 to 55 km derived from our structural interpretation of the Andes is therefore within the range of values obtained independently by crustal-scale area balance. The 71km value proposed by *Giambiagi et al. (2014)* slightly overestimates crustal shortening. We determine that an average mass removal by erosion of ~3 to 12 km of crust over the entire 145 km width of the Andes at the latitude of our study area is needed to compensate for the discrepancy between the ~24-59 km crustal shortening estimated here by area balance and the 71 km shortening proposed by *Giambiagi et al. (2014)*. These values are too high in light of the overall

low finite exhumation within the Andes *(Robinson et al., 2004; Hoke et al, 2014; Riesner, 2017)*. Our structural interpretation is therefore more consistent with independent constraints on shortening estimates, and these findings comfort our results.

By considering a total shortening of ~31-55 km over the last ~20-25 Myr, we get a long-term average shortening rate of ~1.2-2.2 mm/yr across the entire Andes at latitude 33.5°S.

6. Conclusion: kinematics and mechanics of Andean mountain-building at 33.5°S.

The Andes mountain belt at 33.5°S is here described as a bi-vergent orogen, with a dominant primary westward vergence, synthetic to the subduction zone. Indeed, our detailed geological investigations, combined with published data, indicate that the two east-verging structures are secondary or only recent features of Andean mountain-building at 33.5°S latitude, in contrast with most previous interpretations *(e.g. Ramos et al., 2004; Giambiagi et al., 2014)* but consistent with the earlier idea of *Armijo et al (2010)*. Given its relative dimensions and cumulative shortening, its timing of deformation and its structural position within the mountain range (Figure 7), the Aconcagua-FTB appears as a secondary structural feature that passively accommodates Andean deformation (Figure 8). In our model, the thin-skinned Aconcagua-FTB contributed to less than ~30% of the cumulative shortening across the Principal Cordillera. These estimates are based on our non-unique interpretation of the Aconcagua-FTB, using the most simple structural solutions for field observations (Figure 6). Other published interpretations, in particular those implying larger cumulative shortening values across the Aconcagua-FTB are however difficult to reconcile with geological constraints at a regional scale, in particular when accounting for the dimensions and cumulative shortening of nearby thicker-skinned structural ensembles (West Andean-FTB and WVF to the west, and Frontal Cordillera basement antiform to the east), as well as for the overall eastward stratigraphic deepening of surface geology in parallel to eastward increasing topography. Moreover, previous interpretations proposed that the Aconcagua-FTB represented the former mountain front from ~21 to ~10 Ma, before deformation propagated eastward onto the eastern flank of the Frontal Cordillera *(Giambiagi et al., 2003; Ramos et al., 2004; Giambiagi et al., 2014)* (Figure 2a). This view is incompatible with recent thermochronological data on early initiation of exhumation of the Frontal Cordillera basement antiform by ~20-25 Ma (*Hoke et al., 2014, Riesner, 2017)*, i.e. before deformation started within the Aconcagua-FTB but coeval with deformation within the West Andean-FTB *(Riesner et al., 2017)*. Given our results on the structure of the Aconcagua-FTB and on the re-appraisal of its structural position within Andean mountain-building, together with the evidence for an early exhumation of the Frontal Cordillera *(Hoke et al, 2014; Porras et al. 2016)*, we favor a conceptual bi-vergent model, with continuous primary westward deformation of the Andes over the last ~20-25 Myr (Figure 2a). Such model implies that the intra-mountainous basins located between the Aconcagua FTB and the Frontal Cordillera (Figure 3) had not been part of an initial continuous eastern foreland basin as classically viewed *(e.g. Giambiagi et al., 2003; Giambiagi et al., 2014)*, but rather been deposited in between growing adjacent topographic highs. This idea has also been recently proposed by *Hoke et al (2014)* from their thermochronological results, or evoked as a possible interpretation of provenance sources in these intra-mountainous basins by *Porras et al (2016)*.

Within the overall Principal Cordillera, westward vergence is documented within the West Andean-FTB *(Armijo 2010, Riesner et al. 2017)*, the WVF *(Armijo et al., 2010; this study)* but also at a larger scale by the west-vergent large-scale basement antiform of the Frontal Cordillera (Figures 4, 10). Given its dimensions, deformation of the Frontal Cordillera needs to be rooted at depth over a crustal-scale ramp that we propose to connect with the décollement beneath the West Andean-FTB. This mountain range décollement, called the West Andean Thrust (WAT) after *Armijo et al (2010)*, provides the necessary boundary conditions to produce the westward deformation and inversion of the initial Meso-Cenozoic basin of the Principal Cordillera. Within this framework, the topographic high of the Frontal Cordillera basement in the inner part of the orogen supplies the rigid backstop for such westward deformation. Our kinematic evolutionary model (Figure 8) suggests that this backstop is transported westward over the crustal ramp of the WAT, coeval with the outward propagation West Andean-FTB. Existing geophysical data further north and south of our crustal-scale cross-section *(Gilbert et al., 2006)*, as well as at the latitude of our section *(Gans et al., 2011)* are compatible with a

crustal root beneath the west-vergent basement culmination of the Frontal Cordillera, with a Moho depth of ~45-50 km.

Astini and Davila (2010) criticized the bi-vergent model first proposed by *Armijo et al. (2010)* and further discussed in detail here, mainly because of the lack of a prominent foreland basin to the west, in the forearc region, in comparison to a well-developed basin east of the Andes. We first note that latitudinal variations on the eastern side of the Andes are important. At 33.5°S latitude, the Cenozoic sediments of the Cuyo basin are dated from ~16 Ma *(Yrigoyen, 1993; Irigoyen et al., 2000; Garcia and Casa, 2014)*, i.e. after the initiation of the Frontal Cordillera exhumation at ~25 Ma *(Hoke et al., 2014)*. The deformation in the basin is minor, (<5 km) and only recent (<4 Ma) *(Garcia et al., 2005, Garcia and Casa, 2014 and Giambiagi et al., 2015)*. We also note that the existence of an earlier wide continuous foreland basin above the Frontal Cordillera is refuted by *Hoke at al. (2014)*'s results, further limiting the significance of a prominent eastern foreland. Following *Armijo et al. (2010b)*, we understand that the absence - or reduced amplitude - of a western foreland basin may be due 1) to the fact that major rivers drain sediments toward the ocean, and 2) that accretionary and underplating processes at the subduction interface may induce uplift able to counter-act the flexure of the marginal block that underthrusts beneath the Principal Cordillera (Figure 10).

The structural style of deformation of the initial Meso-Cenozoic basin of the Principal Cordillera at 33.5°S seems to be influenced by the inherited structures of the initial basin as well as the distribution of evaporites within its basal décollement. Indeed, we show that the asymmetric geometry of this initial basin may have played a major role in controlling deformation during its subsequent inversion. At a larger scale, a similar reasoning applies to the overall structure of the Andes within our study area by 33.5°S (Figure 10) as the inherited pre-structuration of the western subduction margin of the South America Plate may have largely influenced Andean deformation and subsequent mountain-building. Initiation of deformation along the WAT - and therefore initiation of the intracontinental subduction and underthrusting of the forearc marginal block beneath the South American continent - may have been controlled by mechanical weakening within the volcanic arc. As such, Andean deformation – and in general subduction-type mountain belts - may be further understood in light of the thermo-mechanical analogue models of intra-oceanic arc-continent collision of *Boutelier et al., (2003, 2012)*. In these models, failure of the overriding plate initiates along the volcanic arc in the absence of back-arc basins, and leads to the subduction of a forearc sliver beneath the overriding plate, synthetic to the main subduction zone. Even though these models may not be directly extrapolated to the Andes where the upper plate is constituted of continental crust, the similarity between the modeled and observed structures provide a mechanical framework to further understand mountain-building in the case of subduction orogenies. Thermal weakening and the pre-structuration of the forearc basins favor the initiation of the intracontinental subduction of the forearc block beneath the upper plate, along a crustal-scale décollement synthetic to the major subduction zone. Mountain-building and upper-plate topography here results from the buoyancy and flexure of the underthrust continental forearc. Following this idea, despite the fact that the peculiar boundary conditions of the underthrust forearc prohibit major flexure of the marginal block, probably inducing later east-vergent backthrusts antithetic to the subduction, the kinematics and mechanics of Andean mountain-building - and by extension of cordilleran-type orogenies - can ultimately be compared to that of alpine-type collision mountain belts.

Acknowledgments

Work supported by a PhD grant attributed to M. Riesner by the French Ministry of higher education and research (MESR), and funded by ANR project MegaChile (grant ANR-12-BS06-0004-02) and LABEX UnivEarthS project (Sorbonne Paris Cité, Work Package 1). The manuscript benefitted from the thorough reviews of N. Bellahsen and the critical comments of two anonymous reviewers. The Associate Editor is also warmly thanked for his open-minded scientific handling of this manuscript. All data for 3D mapping measurements carried out as part of this study can be found in the supporting information. This is IPGP contribution N°XXX.

References

Aguirre-Urreta, M.B., 1996. El Tithoniano marino en la vertiente argentina del paso de Piuquenes. 13j Congr. Geológico Argentino. 3j Congr. Explor. Hidrocarburos. Actas, vol. 5, p. 185.

Aguirre-Urreta, M.B., Alvarez, P.P., 1998. Late Jurassic stratigraphy of the High Andes of Argentina and Chile (34 S). 5j Int. Symp. on the Jurassic System, Abstracts: 2, Vancouver.

Aguirre, L., D. Robinson, R. E. Bevins, D. Morata, M. Vergara, E. Fonseca and J. Carrasco (2000), A low-grade metamorphic model for the Miocene volcanic sequences in the Andes of central Chile, New Zealand Journal of Geology and Geophysics, 43:1, 83-93, DOI: 10.1080/00288306.2000.9514871

Alvarado, P., S. Beck, and G. Zandt (2007), Crustal structure of the south-central Andes Cordillera and backarc region from regional waveform modelling, Geophys. J. Int., 170, 858–875, doi:10.1111/ j.1365-246X.2007.03452.x.

Armijo, R., R. Rauld, R. Thiele, G. Vargas, J. Campos, R. Lacassin, and E. Kausel (2010), The West Andean Thrust, the San Ramón Fault, and the seis- mic hazard for Santiago, Chile, Tectonics, 29, TC2007, doi: 10.1029/2008TC002427.

Armijo, R., R. Rauld, R. Thiele, G. Vargas, J. Campos, R. Lacassin, and E. Kausel, (2010b), Reply to the comment by R. A. Astini and F. M. Dávila on ―The West Andean Thrust, the San Ramón Fault, and the seismic hazard for Santiago, Chile‖. Tectonics, 29, TC4010, doi:4010.1029/2010TC002692, doi: 10.1029/2010TC002692.

Armijo, R., Lacassin, Robin, Coudurier-Curveur, Aurélie, Carrizo, Daniel, Coupled tectonic evolution of Andean orogeny and global climate. (2015) Earth Science Reviews doi: 10.1016/j.earscirev.2015.01.005

Astini, R. A., and F. M. Dávila, 2010. Comment on ―The West Andean Thrust, the San Ramón Fault, and the seismic hazard for Santiago, Chile‖ by Armijo et al. Tectonics, 29, TC4009, doi:4010.1029/2009TC002647, doi: doi: 10.1029/2009TC002647.

Beccar, I., M. Vergara, and F. Munizaga (1986), Edades K/Ar de la formación Farellones, en el cordón del cerro La Parva, Cordillera de Los Andes de Santiago, Rev. Geol. Chile, 28–29, 109–113.

Bellahsen N., L. Jolivet, O. Lacombe, M. Bellanger, A. Boutoux, S. Garcia, F. Mouthereau, L. Le Pourhiet, and C. Gumiaux. 2012. Mechanisms of Margin Inversion in the External Western Alps: Implications for Crustal Rheology. Tectonophysics 560, 62–83. doi:10.1016/j.tecto.2012.06.022.

Bellahsen N., F. Mouthereau, A. Boutoux, M. Bellanger, O. Lacombe, L. Jolivet, Y. Rolland. 2014. Collision kinematics in the western external Alps, Tectonics, doi :10.1002/2013TC003453

Bonini, M., 2001, Passive roof thrusting and forelandward fold propagation in scaled brittle–ductile physical models of thrust wedges: Journal of Geophysical Research, v. 106, no. B2, p. 2291–2311.

Boutelier D, Chemenda A, Burg J (2003) Subduction versus accretion of intra-oceanic volcanic arcs: insight from thermo-mechanical analogue experiments. Earth Planet Sci Lett 212(1–2):31–45

Boutelier, D., Oncken, O., Cruden, A., 2012. Fore-arc deformation at the transition between collision and subduction: insights from 3-D thermomechanical laboratory experi- ments. Tectonics 31 (2), 1–15. http://dx.doi.org/ 10.1029/2011TC003060.

Capitanio, F.A., Faccenna, C., Zlotnik, S., and Stegman, D.R., 2011, Subduction dynamics and the origin of Andean orogeny and the Bolivian orocline: Nature, v. 480, no. 7375, p. 83–86, doi: 10.1038/nature10596.

Cegarra, M., Ramos, V.A., 1996. La faja plegada y corrida del Aconcagua, In Geología de la región del Aconcagua, provincias de San Juan y Mendoza (Ramos, V.A.; editor). Subsecretaría de Minería de la Nación, Dirección Nacional del Servicio Geológico, Buenos Aires, Anales 24 (14), 387–422.

Charrier, R., O. Baeza, S. Elgueta, J. J. Flynn, P. Gans, S. M. Kay, N. Muñoz, A. R. Wyss, and E. Zurita (2002), Evidence for Cenozoic extensional basin development and tectonic inversion south of the flat‐slab segment, southern central Andes, Chile (33°–36° S.L.), J. South Am. Earth Sci., 15, 117–139, doi:10.1016/ S0895-9811(02)00009-3.

Charrier, R., M. Bustamante, D. Comte, S. Elgueta, J. J. Flynn, N. Iturra, N. Muñoz, M. Pardo, R. Thiele, and A. R. Wyss (2005), The Abanico extensional basin: Regional extension, chronology of tectonic inversion and relation to shallow seismic activity and Andean uplift, Neues Jahrb. Geol. Palaeontol. Abh., 236, 43–77.

Charrier, R., L. Pinto, and M. P. Rodríguez (2007), Tectonostratigraphic evolution of the Andean Orogen in Chile, in The Geology of Chile, edited by T. Moreno and W. Gibbons, pp. 21–114, Geol. Soc., London.

Dahlen, F. A. (1990), Critical taper model of fold‐and‐ thrust belts and accretionary wedges, Annu. Rev. Earth Planet. Sci., 18, 55–99, doi:10.1146/annurev. ea.18.050190.000415.

Darwin, C. R. (1846), Geological observations on South America. Being the third part of the geology of the voyage of the Beagle, under the command of Capt. Fitzroy, R.N. during the years 1832 to 1836. London: Smith Elder and Co. http://darwin-online.org.uk/content/frameset?pageseq=196&itemID=F273&viewtype=side

Davis, D., J. Suppe, and F. A. Dahlen (1983), Mechanics of fold−and−thrust belts and accretionary wedges, J. Geophys. Res., 88(B2), 1153–1172, doi:10.1029/ JB088iB02p01153.

Davis, D.M., and T. Engelder, The role of salt in fold-and-thrust belts, Tectonophysics 119,67-88,1985.

Deckart, K., A. H. Clark, C. Aguilar, R. Vargas, A. Bertens, J. K. Mortensen, and M. Fanning (2005), Magmatic and hydrothermal chronology of the giant Río Blanco porphyry copper deposit, central Chile: Implications of an integrated U-Pb and 40Ar/39Ar database, Econ. Geol., 100, 905–934, doi:10.2113/100.5.905.

Deville, É., A. Mascle, C. Lamiraux, and A. Le Bras (1994), Tectonic styles, reevaluation of plays in southeastern France, Oil Gas J., 31, 53–58.

Faccenna, C., Becker, T.W., Conrad, C.P., and Husson, L., 2013, Mountain building and mantle dynamics: Tectonics, v. 32, no. 1, p. n/a–n/a, doi: 10.1029/2012TC003176.

Faccenna, C., Oncken, O., Holt, A. F., and Becker, T. W. (2017). Initiation of the andean orogeny by lower mantle subduction. Earth and Planetary Science Letters, 463:189–201.

Farías, M., Comte, D., Charrier, R., Martinod, J., and C. David (2010) Crustal-scale structural architecture in central Chile based on seismicity and surface geology: Implications for Andean mountain building. Tectonics.VOL. 29, TC3006, doi:10.1029/2009TC002480

Fock, A. (2005), Cronología y tectónica de la exhumación en el Neógeno de los Andes de Chile central entre los 33° y los 34° S, Tésis para optar al grado de Magíster en Ciencias, Mención Geología, Memoria para optar al título de Geólogo, thesis, 179 pp., Dep. de Geol., Univ. de Chile, Santiago.

Fock, A., R. Charrier, M. Farías, and M. A. Muñoz (2006), Fallas de vergencia oeste en la Cordillera Principal de Chile Central: Inversión de la cuenca de Abanico, Asociación Geológica Argentina, Serie Publicación Especial, 6, 48-55.

Fromm, R., G. Zandt, and S. Beck (2004), Crustal thickness beneath the Andes and Sierras Pampeanas at 30°S inferred from Pn apparent phase velocities, Geophys. Res. Lett., 31, L06625, doi:10.1029/ 2003GL019231.

Gana, P., D. Sellés, and R. Wall (1999), Mapa geológico area Tiltil−Santiago, región metropolitana, Mapas Geol.11, scale 1:100,000, Serv. Nac. de Geol. y Miner., Santiago.

Gans, C. R., Beck, S. L., Zandt, G., Gilbert, H., Alvarado, P., Anderson, M. and Linkimer, L. (2011), Continental and oceanic crustal structure of the Pampean flat slab region, western Argentina, using receiver function analysis: new high-resolution results. Geophysical Journal International, 186: 45–58. doi:10.1111/j.1365-246X. 2011.05023.x

García, V. H., Cristallini, E. O., Cortés, J. M. & Rodríguez, C. 2005. Structure and neotectonics of the Jaboncillo and Del Peral anticlines: New evidences of Pleistocene to Holocene deformation in the Andean Piedmont. VI International Symposium on Andean Geodynamics, Extended Abstracts, 301 – 304.

García, V. H. & A. Casa (2014). Quaternary tectonics and seismic potential of the Andean retrowedge at 338– 348S. In: Sepulveda, S. A., Giambiagi, L. B., Moreiras, S. M., Pinto, L., Tunik, M., Hoke, G. D. & Farías, M. (eds) Geodynamic Processes in the Andes of Central Chile and Argentina. Geological Society, London, Special Publications, 399. First published online February 27, 2014, http://dx.doi.org/10. 1144/SP399.11

Giambiagi, L. B. (2003), Deformación cenozoica de la faja plegada y corrida del Aconcagua y Cordillera Frontal, entre los 33°30′ y 33°45′S, Asoc. Geol. Argent. Rev., 58, 85–96.

Giambiagi, L.B., Álvarez, P.P., Godoy, E., Ramos, V.A., 2003a. The control of pre-existing extensional structures in the evolution of the southern sector of the Aconcagua fold and thrust belt. Tectonophysics 369, 1–19.

Giambiagi, L. (2000) Estudio de La evolución tectónica de la Cordillera Principal de Mendoza en el sector comprendido entre los 33°30′ y los 33°45′ Latitud Sur (Ph.D. thesis), Universidad de Buenos Aires (255 p).

Giambiagi, L. B., & Ramos, V. A. (2002). Structural evolution of the Andes in a transitional zone between flat and normal subduction (33 30′–33 45′ S), Argentina and Chile. Journal of South American Earth Sciences, 15(1), 101-116.

Giambiagi, L. B., M. Tunik, and M. Ghiglione (2001), Cenozoic tectonic evolution of the Alto Tunuyán foreland basin above the transition zone between the flat and normal subduction segment (33°30′– 34°S), western Argentina, J. South Am. Earth Sci., 14, 707–724, doi:10.1016/S0895-9811(01)00059-1.

Giambiagi, L. B., V. A. Ramos, E. Godoy, P. P. Alvarez, and S. Orts (2003a), Cenozoic deformation and tectonic style of the Andes, between 33° and 34° south latitude, Tectonics, 22(4), 1041, doi:10.1029/ 2001TC001354.

Giambiagi, L., Mescua, J., Bechis, F., Tassara, A., and Hoke, G., 2012, Thrust belts of the southern Central Andes: Along-strike variations in shortening, topography, crustal geometry, and denudation: Geological Society of America Bulletin, v. 124, no. 7-8, p. 1339–1351, doi: 10.1130/B30609.1.

Giambiagi, L., Tassara, A., Mescua, J., Tunik, M., Alvarez, P.P., Godoy, E., Hoke, G., Pinto, L., Spagnotto, S., Porras, H., Tapia, F., Jara, P., Bechis, F., Garcia, V.H., et al., 2014, Evolution of shallow and deep structures along the Maipo-Tunuyan transect (33 40'S): from the Pacific coast to the Andean foreland: Geological Society London Special Publications, 2014, doi: 10.1144/SP399.14.

Giambiagi, L., Spagnotto, S., Moreiras, S. M., Gómez, G., Stahlschmidt, E., & Mescua, J. (2015). Three-dimensional approach to understanding the relationship between the Plio-Quaternary stress field and tectonic inversion in the Triassic Cuyo Basin, Argentina. Solid Earth, 6(2), 747.

Gilbert, H., S. Beck, and G. Zandt (2006), Lithospheric and upper mantle structure of central Chile and Argentina, Geophys. J. Int., 165, 383–398, doi:10.1111/j.1365-246X.2006.02867.x.

Godoy, E., Harrington, R., Fierstein, J., & Drake, R. (1988). El Aconcagua¿ parte de un volcan mioceno?. Andean Geology, 15(2), 167-172.

Graveleau, F., Malavieille, J., and Dominguez, S., 2012, Experimental modelling of orogenic wedges: A review: Tectonophysics, v. 538-540, no. C, p. 1–66, doi: 10.1016/j.tecto.2012.01.027.

Gregori, D.A., Fernández-Turiel, J.L., López-Soler, A., Petford, N., 1996. Geochemistry of Upper Palaeozoic-Lower Triassic granitoids of the Central Frontal Cordillera (33_10'-33_45'), Argentina. Journal of South American Earth Sciences 9, 141e151.

Groeber, P., 1918. Estratigrafia del Dogger en la Repfblica Ar- gentina. Estudio sint6tico comparativo. Dir. Gen. Minas Geol. Hidrogeol. Bol. Ser. B (Geol.), 18: 1-81.

Gwinn, V.E., Thin-skinned tectonics in the Plateau and Northwestern Valley and Ridge Provinces of the Central Appalachian, Geol. Soc. Am. Bull., 75, 863-900, 1964.

Heredia, N., Farias, P., García Sansegundo, J., and Giambiagi, L., 2012, The Basement of the Andean Frontal Cordillera in the Cordón del Plata (Mendoza, Argentina): Geodynamic Evolution: Andean geology, v. 39, no. 2, p. 242–257.

Hoke, G. D., N. R. Graber, J. F. Mescua, L. B. Giambiagi, P. G. Fitzgerald, and J. R. Metcalf, 2014. Near pure surface uplift of the Argentine Frontal Cordillera: insights from (U–Th)/He thermochronometry and geomorphic analysis. in Geodynamic Processes in the Andes of Central Chile and Argentina, edited by S. A. Sepúlveda, et al., doi: 10.1144/SP399.4, Geological Society, London, Special Publications.

Husson, L., Conrad, C.P., and Faccenna, C., 2012, Plate motions, Andean orogeny, and volcanism above the South Atlantic convection cell: Earth and Planetary Science Letters, v. 317-318, no. C, p. 126–135, doi: 10.1016/j.epsl.2011.11.040.

Introcaso, A., M. C. Pacino, and H. Fraga (1992), Gravity, isostasy and Andean crustal shortening between latitudes 30 and 35°S, Tectonophysics, 205(1–3), 31–48, doi:10.1016/0040-1951(92)90416-4.

Irigoyen, M. V., K. L. Buchan, and R. L. Brown (2000), Magnetostratigraphy of Neogene Andean foreland basin strata, lat 33°S, Mendoza Province, Argentina, Geol. Soc. Am. Bull., 112, 803–816, doi:10.1130/0016-7606(2000)112<0803:MONAFB>2.3.CO;2.

Isacks, B. L. (1988). Uplift of the central andean plateau and bending of the bolivian orocline. Journal of Geophysical Research: Solid Earth, 93(B4):3211–3231.

James, D. E. (1971). Andean crustal and upper mantle structure. Journal of Geophysical Research, 76(14):3246–3271.

Kley, J., 1999. Geologic and geometric constraints on a kinematic model of the Bolivian orocline. J. S. Am. Earth Sci. 12 (2), 221–235.

Kono, M., Fukao, Y., and Yamamoto, A. (1989). Mountain building in the central andes. Journal of Geophysical Research: Solid Earth, 94(B4):3891–3905.

Lacombe, O., & Bellahsen, N. (2016). Thick-skinned tectonics and basement-involved fold–thrust belts: insights from selected Cenozoic orogens. Geological Magazine,143, 1-48, doi:10.1017/S0016756816000078

Lafosse, M., Boutoux, A., Bellahsen, N., & Le Pourhiet, L. (2016). Role of tectonic burial and temperature on the inversion of inherited extensional basins during collision. Geological Magazine, 153(5-6), 811-826.

Lamb, S. (2011). Did shortening in thick crust cause rapid late cenozoic uplift in the northern bolivian andes? Journal of the Geological Society, 168(5):1079–1092.

Leloup, P., Arnaud, N., Sobel, E., and Lacassin, R., 2005, Alpine thermal and structural evolution of the highest external crystalline massif: The Mont Blanc: Tectonics, doi:10.1029/2004TC001676.

Llambías, E. J., S. Quenardelle, and T. Montenegro (2003), The Choiyoi Group from central Argentina: A subalkaline transitional to alkaline association in the craton adjacent to the active margin of the Gondwana continent, J. South Am. Earth Sci., 16, 243–257, doi:10.1016/S0895-9811(03)00070-1.

Lo Forte, G.L., 1992. Evolución Paleogeografica del Mesozoico Marino de la Región del Aconcagua. Doct. Thesis, Univ. Buenos Aires, 302 pp. (unpubl.).

Lyon-Caen, H., Molnar, P., and Suárez, G. (1985). Gravity anomalies and flexure of the brazilian shield beneath the bolivian andes. Earth and Planetary Science Letters, 75(1):81–92.

Malavieille, J. (1984). Modélisation expérimentale des chevauchements imbriqués: application aux chaînes de montagnes. Bulletin de la Société géologique de France, 26(1), 129-138.

McClay, K., and Whitehouse, P.S., 2004, Analog modeling of doubly vergent thrust wedges: AAPG Memoir, v. 82, p. 184–206.

McQuarrie, N., Horton, B. K., Zandt, G., Beck, S., and DeCelles, P. G. (2005). Lithospheric evolution of the andean fold–thrust belt, bolivia, and the origin of the central andean plateau. Tectonophysics, 399(1):15–37.

Molnar, P., & Atwater, T. (1978). Interarc spreading and Cordilleran tectonics as alternates related to the age of subducted oceanic lithosphere. Earth and Planetary Science Letters, 41(3), 330-340.

Mouthereau,F., P.-Y.Filleaudeau, A.Vacherat, R.Pik, O.Lacombe, M.G.Fellin, S. Castelltort, F. Christophoul, and E. Masini (2014), Placing limits to shortening evolution in the Pyrenees: Role of margin architecture and implications for the Iberia/Europe convergence, Tectonics, 33, 2283–2314, doi:10.1002/2014TC003663.

Mpodozis, C., and V. A. Ramos (1989), The Andes of Chile and Argentina, in Geology of the Andes and Its Relation to Hydrocarbon and Mineral Resources, Earth Sci. Ser., vol. 11, edited by G. E. Ericksen, M. T. Cañas Pinochet, and J. A. Reinemund, pp. 59–90, Circum Pac. Counc. for Energy and Miner Resour., Houston, Tex.

Nieuwland, D. A., Leutscher, J. H., & Gast, J. (2000). Wedge equilibrium in fold-and-thrust belts: prediction of out-of-sequence thrusting based on sandbox experiments and natural examples. Geologie en Mijnbouw/ Netherlands Journal of Geosciences, 79 (1), 81-91.

Nieuwland, D. A., Oudmayer, B.C., and Valbona, U. (2001). The tectonic development of Albania: explanation and prediction of structural styles. Marine and Petroleum Geology 18 161-177.

Nyström, J. O., M. Vergara, D. Morata, and B. Levi (2003), Tertiary volcanism during extension in the Andean foothills of central Chile (33°15′–33°45′S), Geol. Soc. Am. Bull., 115, 1523–1537, doi:10.1130/B25099.1.

Oncken, O., Boutelier, D., Dresen, G., and Schemmann, K. (2013). Strain accumulation controls failure of a plate boundary zone: Linking deformation of the central andes and lithosphere mechanics. Geochemistry, Geophysics, Geosystems, 13(12).

Oncken, O., Hindle, D., Kley, J., Elger, K., Victor, P., and Schemmann, K. (2006). Deformation of the central andean upper plate system—facts, fiction, and constraints for plateau models. In The Andes, pages 3–27. Springer.

Polanski, J. (1964), Carta geológico económica de la República Argentina escala 1:200000, Hoja 25 a–b– Volcán de San José, provincia de Mendoza. Descripción geológica de la hoja, Bol. 98, pp. 1–92, Dir. Nac. de Geol. y Min., Buenos Aires.

Polanski, J. (1972), Carta Geológico Económica de la República Argentina escala 1:200,000, Hoja 24 a–b– Cerro Tupungato, provincia de Mendoza. Descripción geológica de la hoja, Bol. 128, pp. 1–110, Dir. Nac. de Geol. y Min., Buenos Aires.

Porras, H., Pinto, L., Tunik, M., Giambiagi, L., & Deckart, K. (2016). Provenance of the Miocene Alto Tunuyán Basin (33° 40′ S, Argentina) and its implications for the evolution of the Andean Range: Insights from petrography and U–Pb LA–ICPMS zircon ages. Tectonophysics, 690, 298-317

Ramos, V.A., 1985. E1 Mesozoico de la Alta Cordillera de Mendoza: reconstrucci6n tect6nica de sus facies, Argentina. IV Congr. Geol. Chil., Antofagasta, Actas, 1(2): 104-118,

Ramos, V.A., 1988. The tectonics of the Central Andes 30° to 33°S latitude, in Processes in Continental Lithospheric Deformation, Clark, S., Burchfiel, D. (Eds.), Geological Society of America, Special Paper 218, 31–54.

Ramos, V. A., M. L. Cegarra, and E. Cristallini (1996a), Cenozoic tectonics of the High Andes of west/central Argentina (30°–36°S latitude), Tectonophysics, 259, 185–200, doi:10.1016/0040-1951 (95)00064-X.

Ramos, V.A.; Cegarra, M.I.; Pérez, D.J. (1996b). Carta Geológica, Región del Aconcagua. In Geología de la región del Aconcagua, provincias de San Juan y Mendoza (Ramos, V.A.; editor). Subsecretaría de Minería de la Nación, Dirección Nacional del Servicio Geológico, Buenos Aires, Anales 24.

Ramos, V.A.; Cegarra, M.I.; Pérez, D.J. (1996c). El volcanismo de le región del Aconcagua. In Geología de la región del Aconcagua, provincias de San Juan y Mendoza (Ramos, V.A.; editor). Subsecretaría de Minería de la Nación, Dirección Nacional del Servicio Geológico, Buenos Aires, Anales 24 (10), 297-316.

Ramos, V., 1999, Rasgos estructurales del territorio Argentino 1. Evolution Tectonica de la Argentina: Geologia Argentina, v. 24, p. 715–784.

Ramos, V.A., Cristalini, E.O. & Perez, D.J. 2002. The Pampean flat-slab of the Central Andes. Journal of South American Earth Sciences 15(1), 59–78.

Ramos, V. A., T. Zapata, E. Cristallini, and A. Introcaso (2004), The Andean thrust system—Latitudinal var- iations in structural styles and orogenic shortening, in Thrust Tectonics and Hydrocarbon Systems, edi- ted by K. R. McClay, AAPG Mem., 82, 30–50.

Ramos, V., 2010, The tectonic regime along the Andes: Present-day and Mesozoic regimes: Geological Journal, v. 45, no. 1, p. 2–25.

Riesner, M., R. Lacassin, M. Simoes, R. Armijo, R. Rauld, and G. Vargas (2017), Kinematics of the active West Andean fold-and-thrust belt (Central Chile): structure and long-term shortening rate, Tectonics, 36, doi: 10.1002/2016TC004269.

Riesner, M. (2017), Evolution tectonique des Andes centrales (33°S): implications sur la mécanique des chaînes de subduction. PhD thesis. Institut de Physique du Globe de Paris, 205pp.

Rivano, S.; Sepúlveda, P;, Boric, R.; Espiñeira, D. 1993. Hojas Quillota y Portillo, Escala 1:250.000: Santiago, Servicio Nacional de Geología y Minería, Carta Geológica de Chile, n° 73.

Robinson, D., R. Bevins, L. Aguirre, and M. Vergara (2004), A reappraisal of episodic burial metamor- phism in the Andes of central Chile, Contrib. Mineral. Petrol., 146, 513–528, doi:10.1007/s00410- 003-0516-4.

Russo, R., Silver, P., et al. (1994). Trench-parallel flow beneath the nazca plate from seismic anisotropy. SCIENCE-NEW YORK THEN WASHINGTON-, pages 1105–1105.

Schellart, W. P., J. Freeman, D. R. Stegman, L. Moresi, and D. May, 2007. Evolution and diversity of subduction zones controlled by slab width. Nature, 446, 308-311, doi: 10.1038/nature05615.

SEGEMAR (2000), Carta Geológica a escala 1:250.000, Hoja 3369-I Cerro Aconcagua, Instituto de Geología y Recursos Minerales, Servicio Geológico Minero Argentino, Buenos Aires.

SEGEMAR (2010), Carta Geológica a escala 1:250.000, Hoja 3369-III Cerro Tupungato, Instituto de Geología y Recursos Minerales, Servicio Geológico Minero Argentino, Buenos Aires.

SERNAGEOMIN, 2003. Mapa Geológico de Chile: versión digital. Servicio Nacional de Geología y Minería, Publicación Geológica Digital, No. 4 (CD-ROM, versión1.0, 2003). Santiago.

Suárez, G., Molnar, P., Burchfiel, B.C., 1983. Seismicity, fault plane solutions, depth of faulting, and active tectonics of the Andes of Peru, Ecuador, and southern Colombia. J. Geophys. Res. 88 (B12), 10403–10428.

Tapponnier, P., X. Zhiqin, F. Roger, B. Meyer, N. Arnaud, G. Wittlinger, and Y. Jingsui (2001), Oblique stepwise rise and growth of the Tibet Plateau, Science, 294, 1671–1677, doi:10.1126/ science.105978.

Tassara, A., H. J. Götze, S. Schmidt, and R. Hackney (2006), Three-dimensional density model of the Nazca plate and the Andean continental margin, J. Geophys. Res., 111, B09404, doi:10.1029/ 2005JB003976.

Thiele, R. (1980), Geología de la hoja Santiago, Región Metropolitana, Carta Geológica de Chile, scale 1:250,000, pp. 51, Inst. de Invest. Geol., Santiago.

Vargas, G. ,Y. Klinger, T.K. Rockwell, S.L. Forman, S. Rebolledo, S. Baize, R. Lacassin and R. Armijo (2014). Probing large intraplate earthquakes at the west flank of the Andes, Geology. doi:10.1130/G35741.1

Vergara, M., R. Charrier, F. Munizaga, S. Rivano, P. Sepulveda, R. Thiele, and R. Drake (1988), Miocene volcanism in the central Chilean Andes (31°30′S–34°35′S), J. South Am. Earth Sci., 1, 199–209, doi: 10.1016/0895-9811(88)90038-7.

Vergara, M., L. López-Escobar, J. L. Palma, R. Hickey and Vargas, and C. Roeschmann (2004), Late tertiary volcanic episodes in the area of the city of Santiago de Chile: New geochronological and geochemical data, J. South Am. Earth Sci., 17, 227–238, doi:10.1016/j.jsames.2004.06.003.

Yrigoyen, M. R. 1993. Los depósitos sinorogénicos terciarios. In: Ramos, V. A. (ed.) Geología y recursos naturales de la Provincia de Mendoza, Mendoza, Argentina, 123–148.

Willett, S., C. Beaumont, and P. Fullsack (1993), Mechanical model for the tectonics of doubly vergent compressional orogens, Geology, 21, 371–374, doi:10.1130/0091-7613(1993)021<0371: MMFTTO>2.3.CO;2.